DISSERTATION

On

MODEL REDUCTION IN VEHICLE DYNAMIC SYSTEMS

Submitted in partial fulfilment of the requirement for the award of degree

of

Master of Engineering

IN

CAD/CAM Engineering

Submitted by

Manarshhjot Singh

Roll No.: 801381010

Under the Supervision of

Dr. Tarun Kumar Bera

Department of Mechanical Engineering

Thapar University, Patiala

DEPARTMENT OF MECHANICAL ENGINEERING

THAPAR UNIVERSITY

PATIALA-147004, INDIA

JULY-2015

DECLARATION

I hereby declare that work done in this seminar report entitled, "**Model Reduction in Vehicle Dynamic Systems**" submitted towards partial fulfilment of requirement for award of **Master of Engineering degree** in **CAD/CAM Engineering** in **Mechanical Engineering Department** of **Thapar University, Patiala**, is an authentic record of work carried out by me under the supervision and guidance of **Dr. Tarun Kumar Bera, Associate Professor** of **Mechanical Engineering Department, Thapar University, Patiala.**

This matter embodied in this report has not been submitted in part or full to any other university or institute for the award of any degree.

MANARSHHJOT SINGH

This is to certify that above declaration made by the student concerned is correct to the best of my knowledge and belief.

Tarun Kumar Bera 15/7/15

Dr. Tarun Kumar Bera
Associate Professor
Mechanical Engineering Department
Thapar University, Patiala.

Countersigned by:

Head of ME Department,
Thapar University, Patiala.

Dean of Academic Affairs,
Thapar University, Patiala.

ACKNOWLEDGEMENT

Words often fall short to reveal one's deepest regards. Understanding that a work like this can never be accompanied by the efforts of a single person, I would be obliged to express my profound gratitude and respect to all the people who helped me throughout the duration of this work.

I would like to thank my supervisor, Dr. Tarun Kumar Bera, Associate Professor, Mechanical Engineering Department, Thapar University, Patiala for his unreserved guidance, constructive suggestions, thought provoking discussions and unabashed inspiration in the nurturing work. He also provided the help in technical writing and presentation style and I found his guidance to be extremely valuable.

I am also Dr. S. K. Mohapatra, Sr. Professor and Head, Mechanical Engineering Department for providing the facilities for the completion of work.

Finally, I am grateful to my family and friends, without their encouragement, patience and moral support, it would not have been possible for me to complete my thesis.

Manarshhjot Singh

Reg. No. 801381010

ABSTRACT

In the future there will be a great demand for autonomous vehicles. New companies like Google and premier automotive companies like Volkswagen have already reached the prototyping stage. Dynamic system plays a crucial role in the monitory success of an automobile project. The autonomous vehicles are guided by complex algorithms, which utilize the data from the sensors to monitor the environment and plan the motion of the car. For predicting the future position and orientation of the vehicle relative to the changing environment, a mathematical model describing the dynamic characteristics of the vehicle needs to be solved. The solution is found by solving the model numerically by iteration process. Hence, the process of solving the model is the bottleneck for the whole process. By reducing the time consumed to solve the model, the cycle time for the overall process can be decreased thus increasing the cycle frequency and hence the performance of the vehicle. The work done in the thesis attempts to achieve this by mathematically finding the redundant elements, which do not add to the dynamics of the system but increase the calculation time by increasing the complexity of the system. Such elements could be neglected from the system and hence reducing the complexity without compromising on the accuracy.

Keywords: Physical model reduction, vehicle dynamics, ABS, eigenvalue separation, eigenvalue sensitivity, bond graph

LIST OF ABBREVIATIONS

ABS	Antilock braking system
C	Compliance element
DOF	Degrees of freedom
G_{CR}	Loop gain between a C and an R element
G_{IC}	Loop gain between an I and a C element
G_{IR}	Loop gain between an I and an R element
GY	Gyrator
I	Inertial element
J_{LL}	Connectivity matrix form output of energy dissipating elements to input of other energy dissipating element
J_{LS}	Connectivity matrix form output of energy storing elements to input of energy dissipating element
J_{SL}	Connectivity matrix form output of energy dissipating elements to input of energy storing element
J_{SS}	Connectivity matrix form output of energy storing elements to input of other energy storing element
LTI	Linear time-invariant
MGY	Modulated gyrator
MIMO	Multi input multi output
MTF	Modulated transformer
MORA	Model reduction algorithm
PID	Proportional-integral-derivative
R	Resistance element
SISO	Single input single output
TF	Transformer

NOMENCLATURE

a	Distance of the front suspension point from vehicle center of mass measured along x-direction
b	Distance of the rear suspension point from vehicle center of mass measured along x-direction
c	Distance of the suspension points from vehicle center of mass measured along y-direction
d	Steering angle
e	Generalized effort
f	Generalized flow
g	Acceleration due to gravity
h	Distance of the suspension points from vehicle center of mass measured along z-direction
l_a	Length of arm in ABS
l_i	i^{th} energy dissipating element
m	Generalized mass
r	Radius
s_i	i^{th} energy storing element
x, y, z	Generalized direction vectors of the non-inertial reference frame
Ef_I	Sensitivity matrix for I-elements in the system
Ef_C	Sensitivity matrix for I-elements in the system
Ef_R	Sensitivity matrix for I-elements in the system
F_i	Force in i-direction
G_i	Loop gain of the i^{th} causal loop
J_{ij}	Moment of inertial of system i, about axis j
L	Characteristic matrix for energy dissipating elements
M_i	Mass of i^{th} system
M_x, M_y, M_z	Moment about x, y and z direction
S	Characteristic matrix for energy storing elements
X, Y, Z	Generalized direction vectors of the inertial reference frame
δ	Average steering angle

δ_i	Steering angle for the inner front wheel
δ_o	Steering angle for the outer front wheel
θ	Rotation angle about y-axis
φ	Rotation angle about x-axis
ψ	Rotation angle about z-axis
ω	Angular velocity

SUBSCRIPTS

c	Vehicle body
r	Rolling
stx	Rotation about x
sty	Rotation about y
stz	Rotation about z
sx	Translation in x
sy	Translation in y
sz	Translation in z
t	Tire sidewalls
w	Wheel
CR	Loop containing a C-element and an R-element
IC	Loop containing an I-element and a C-element
IR	Loop containing an I-element and an R-element

LIST OF FIGURES

LIST OF TABLES

TABLE OF CONTENTS

CHAPTER 1 INTRODUCTION

Simulation of various systems before their actual production is a very important part of the design process. But now due to the application of various new forms of control techniques and algorithms, the need of simulation does not end with the design process. Today many complex systems are controlled by powerful algorithms which continuously monitor the system surroundings and simulate the system on the go. This simulation allows the algorithms to predict and hence control the system in a better manner, with more accuracy. Most of the control algorithms have mathematical equations which can only be solved numerically, and not analytically. As numerical methods are iterative algorithms, a complex system increases the simulation time drastically. Hence, a complex system is difficult to handle for controller design, optimization, computation and storage requirements

1.1 BACKGROUND AND MOTIVATION

An approach to overcome the obstacles of high computation time and cost requirements is to obtain a reduced model of the system, without compromising on the accuracy. Hence, such a mathematical model can be solved quickly and the response characteristics for the reduced model have minimum error compared to the full model. So, model reduction methods have been studied since long time.

There are two major advantages of using a reduced model for control system are

1) It reduces the problem to a smaller manageable size. Hence, the model has less storage and computational requirements.
2) With controller order reduction, we can obtain simpler controllers which are simpler in hardware/software and hence cost effective.

The vehicle dynamic model is a set of equations that can be solved to find out the dynamic characteristics of the vehicle during motion. It is a very important field of study for automotive engineers as it allows them to study and to predict the safety, performance and comfort characteristics of the vehicle. As this study concerns the safety of the passengers in the vehicle, controller design for vehicle dynamics is a very important aspect in designing of automobiles. The antilock braking system (ABS) is a very good example for a controller for such a system. As vehicle dynamics model is a very complex, it is solved numerically. Hence, this numerical method also suffers from the same problems as discussed previously. So, obtaining a quick model which also conserves the dynamics of the systems is very critical. The motivation for designing reduced vehicle models is that it can decrease the computational time for solving the dynamic model and hence, can be used in autonomous

vehicles which can predict and control the behavior of system by continuous monitoring of the environment.

1.2 MODEL ORDER REDUCTION

Traditionally model reduction has been done mathematically. The approach was to first solve the full system, and then obtain a reduced system by mathematical computation. This reduced model was saved for future use. Whenever there was a need for quick model, the saved model was used. Two, important techniques used for mathematical reduction are as follows:

1) Singular Value Decomposition methods [**1**]
2) Moment matching methods [**2**]

1.2.1 Singular value decomposition method

The singular value decomposition methods make use of coordinate transformation technique. A transformation matrix A, which contains the characteristics of the dynamic system can be split into 3 singular values *U*, *S* and *V* such that

$$A = USV^T \tag{1.1}$$

Here *U* and *V* are rotation matrices, containing the left and right singular vectors of the system and S is a scaling matrix, which contains the system singular values of the system as the entries of the diagonal.

The left singular vectors are the eigenvectors of AA^{T}. The right singular vectors are the eigenvectors of $A^{\mathrm{T}}A$.

$$S = diag(\sigma_1,\ \sigma_2,\ \sigma_3, \dots, \sigma_n) \tag{1.2}$$

The matrix *A* can be written in the form described by Eq. (1.3)

$$A\ =\ \sigma_1 u_1 v_1^T\ +\ \sigma_2 u_2 v_2^T\ +\ \cdot\ \cdot\ \cdot\ \sigma_r u_r v_r^T \tag{1.3}$$

where r is the rank of matrix *A*

For the complete transformation the system is first rotated into an intermediate space. Here the system is scaled into the desired form according to the requirements and then rotated into the desired space.

1.2.2 Moment Matching Method

Moment matching methods use approximation methods by truncating the expanded form of a system till a certain level.

Suppose a system is given by transfer function

$$G(s) =\ C\ (\ sI - A\ )^{-1}\ B + D \tag{1.4}$$

The transfer function can be expanded in the form of Laurent Series around the point $s_0 \in C$

$$G\,(\,s_0 + \ \sigma\,) = \eta_0 + \eta_1\sigma + \eta_2\sigma^2 + \eta_3\sigma^3 + \cdots \quad (1.5)$$

η_t are called the moments of s at s_0

A reduced system S' can be given by

$$G'(\,s_0 \ + \ \sigma\,) = \eta'_0 + \eta'_1\sigma + \eta'_2\sigma^2 + \eta'_3\sigma^3 + \cdots \quad (1.6)$$

Where the first k moments are matched i.e.

$$\eta_j = \eta'_j \; for \; j = 1,2,3 \ldots, k \quad (1.7)$$

If s_0 is taken to be ∞, then the problem is called Padé approximation.

1.3 BOND GRAPH MODELLING

Bond graph modelling technique was developed in 1959, by Prof. H.M. Paynter at MIT. The idea was to utilise the law of conservation of energy to develop a generalised technique capable of representing systems from different domains. The technique was developed by introducing seven typed of elements i.e. I, C, R, Se, Sf, TF, GY that could interact with the system represented by two types of junctions i.e. 1-junction and 0-junction. All types of systems could be represented using these seven basic elements. As there were only seven types of elements, the system could easily be solved using simple algorithms. The power flowing through the system analysed. Different elements in the system behave differently with the system and with each other. The power flowing in the system is represented as product of two components, an effort and a flow. Each bond, which symbolises flow of power form one element of a system to another, has a flow and an effort associated with it. The parameters represented by flow variable and the effort variable for different systems are listed in Table 1.1.

Table 1.1: Effort and flow variables in different energy domains [**3**]

Systems	**Efforts (e)**	**Flow (f)**
Mechanical	Force (N)	Velocity (m/s)
	Torque (N-m)	Angular velocity (rad/s)
Electrical	Voltage (V)	Current (A)
Thermal	Temperature (K)	Entropy change rate (W/K)
	Pressure (N/m^2)	Volume change rate (m^3/s)
Hydraulic	Pressure (N/m^2)	Volume flow rate (m^3/s)
Chemical	Chemical potential (Nm/mol)	Mass flow rate (mol/s)
	Entropy (Q/K)	Mass flow rate (kg/s)
Magnetic	Magnetic-motive force (e_m)	Magnetic flux rate (Wb/s)

1.3.1 Parts of bond graph

The basic elements used for representing a system using bond graph technique are I, C, R, Se, Sf, TF and GY. A line segment called bond through which all elements are connected. This bonds represents flow of power i.e., effort information and flow information.

Bond graph model can be classified are as follows:

- Single port passive elements i.e., inertial element (I), compliance element (C) and resistive element (R).
- Single port active elements or source elements i.e., source of effort (SE) and source of flow (SF).
- Multi-port conversion elements i.e., Gyrator (GY) and transformer (TF).
- Junction elements i.e., flow summing junction (0) and effort summing junction (1).

1.3.2 Single-port elements

Single port elements are the elements which are connected to the system on only one point. These can be active or passive. Active elements are those which are the source of power to the system. Passive elements are the elements which only interact with the power in the system. Single port elements are discussed as follows:

- Compliance element: The compliance element is represented by a character 'C'. This bond is further connected to a junction element representing a point in the system. This is an energy storage element. The integral causality is only preferable. The graphical representation of compliant element as shown in Fig. 1.1.

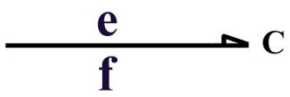

Fig. 1.1 Bond Graph representation of compliance element

$$F = k.x \tag{1.8}$$

$$e = k.Q \tag{1.9}$$

$$e = k \int_{\infty}^{t} f(t)dt \tag{1.10}$$

From Eq. (1.8) and (1.9), it is observed that the integral causality is observed if the output from the element is effort and the input to the element is flow.

- Inertial element: Inertial element is represented by 'I' in the bond graph. This is also an energy storage element. This element gives the relationship between the effort and the flow in such a way that the integration of effort gives the flow. The graphical representation of inertial element is shown in Fig. 1.2.

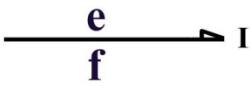

Fig. 1.2 Bond Graph representation of inertial element

$$F = m\ddot{x} = \frac{df}{dt} \times \text{ m} \tag{1.11}$$

$$f = \frac{1}{m}\int_{\infty}^{t} e dt \tag{1.12}$$

$$= \text{k} + \frac{1}{m}\int_{\infty}^{t} e dt \tag{1.13}$$

From Eq. (1.11–1.13), it is observed that the integral causality is observed if the output from the element is flow and the input to the element is effort.

- Resistive element: Resistive element is represented by 'R' in the bond graph. Unlike I and C elements, R-element is en energy dissipater. The graphical representation of resistive element as shown in Fig. 1.3. R-element can have integral causality for any type of input.

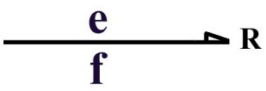

Fig. 1.3 Bond Graph representation of resistive element

- Source of effort: Source of effort is represented by 'SE' in the bond graph. It gives power to the system and in the form of external effort acting on the system. The example of source of effort in mechanical system is force. The graphical representation is shown in Fig. 1.5.

Fig. 1.4 Bond Graph representation of source of effort element

- Source of flow: Source of flow is represented by 'SF' in the bond graph. It gives power to the system and in the form of external flow to system. The example of source of effort in mechanical system is force. The graphical representation is shown in Fig. 1.5.

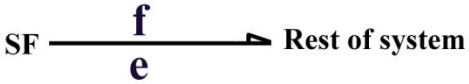

Fig. 1.5 Bond Graph representation of source of flow element

1.3.3 Basic 2 -port elements

Two port elements are elements which are connected to two points on the system. These elements are basically converters which redistribute amount of flow and effort, between the two points that they are connected to. The basic 2-port elements are 'transformer and the gyrator'. The symbolic representation of transformer is 'TF' and gyrator is 'GY'..

- Transformer: Transformer does not create nor destroys energy. They redistribute the amount of flow and effort information. The transformer element magnifies the flow from input side to provide us with the flow on the output side of the element.

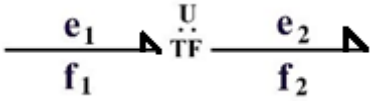

Fig. 1.6 Bond Graph representation of transformer element

$$f_2 = \mu \cdot f_1 \tag{1.14}$$

$$e_1 \cdot f_1 = e_2 \cdot f_2 \tag{1.15}$$

$$\therefore e_2 = \frac{1}{\mu} e_1 \tag{1.16}$$

From Eq. (1.14)-(1.16), it is observed that as power in always conserved, there is also a relation between the input and output effort. As the transformer converts flow to flow and effort to effort the causal direction is not changed when the power flows through a transformer.

- Gyrator: Gyrator does not create nor destroys energy. It redistributes the amount of flow and effort information. The gyrator element magnifies the flow from input side to provide us with the effort on the output side of the element.

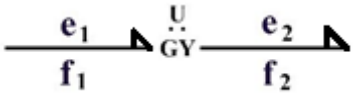

Fig. 1.7 Bond Graph representation of gyrator element

$$e_2 = \mu \cdot f_1 \tag{1.17}$$

$$e_1 \cdot f_1 = e_2 \cdot f_2 \tag{1.18}$$

$$e_1 = \mu \cdot f_2 \tag{1.19}$$

From Eq. (1.17)-(1.19), it is observed that as power in always conserved, there is also a relation between the input effort and output flow. As the gyrator converts

flow to effort and effort to flow the causal direction is changed when the power flows through a gyrator.

1.3.4 Junction Elements

The junctions are of two types, 0-junction and 1-junction. The junctions represent points on the system where other elements can connected. Power is distributed among the connected elements but the nature of distribution depends on the type of junction.

- 1-Junction: 1 junction represents equality of flow. Suppose power comes to a 1-junction through a bond ‘a’ and leaves the junction through ‘b’ and ‘c’.

$$p_a = p_b + p_c \tag{1.20}$$

$$e_a f_a = e_b f_b + e_c f_c \tag{1.21}$$

As flows are equal

$$e_a = e_b + e_c \tag{1.22}$$

From Eq. (1.20)–(1.22), it is observed that for power to be conserved, 1-junction is also an effort sum junction.

- 0-Junction: 0-junction represents equality of effort. Suppose power comes to a 0-junction through a bond ‘a’ and leaves the junction through ‘b’ and ‘c’.

$$p_a = p_b + p_c \tag{1.20}$$

$$e_a f_a = e_b f_b + e_c f_c \tag{1.21}$$

As efforts are equal

$$f_a = f_b + f_c \tag{1.22}$$

From Eq. (1.20)–(1.22), it is observed that for power to be conserved, 0-junction is also a flow sum junction

1.4 VEHICLE DYNAMICS

A vehicle either moving or stationary can be stable or unstable. The vehicle control may be quick and responsive to the driver or it may lag the driver input. Also, in some case the vehicle may experience some changes in trajectory because of external inputs like bump steering effect. A properly designed vehicle satisfies all the concerns of safety, handling, ride *etc*. For vehicle to achieve this, dynamic test should be simulated for the vehicle. The simulation of vehicle is usually concerned with the longitudinal and lateral dynamics of the

vehicle. The other major concerns are the roll, pitch and yaw motion of the vehicle during various scenarios. There are many factors which affect the dynamics of a vehicle, primary of which are load distribution, roll axis, suspension geometry, steering ratio, tire-road characteristics, suspension parameters *etc*.

There are many models which are used for simulating the performance of the vehicle. The models are broadly divided into four types, quarter car model, bicycle model, half car model and four wheel model.

- Quarter car model: The quarter car model is the simplest model used to simulate a vehicle dynamic system. The model basically consists of simulating only one wheel and the suspensions attached to that wheel. The suspensions are loaded with one-fourth the vehicle mass. The model can simulate the very basic straight line motions of very basic suspension characteristics and response.
- Bicycle model: The bicycle model simulates one half of the vehicle, divided along its longitudinal axis. The bicycle model assumes that the mass is equally distributed among both the halves. Hence, only half of the mass of the vehicle is used for simulation. The bicycle model can be of two types depending on the plane in which it is simulated. The bicycle model in the horizontal plane can be used to simulate the motion of the vehicle during steering. Such a model assumes that there is no lateral load transfer. The bicycle model can also be used in the vertical plane. Such a vehicle can be used to simulate the vehicle straight line motion during a hill climb or descent, where suspension characters are important. The model consists of the front and rear tire along with the suspensions attached and the vehicle body, which as in previous case is assumed to have symmetric mass distribution about the longitudinal axis. The model can be used to simulate the load transfer to the front and rear tires, and the pitching motion of the vehicle.
- Half-car model: Half car model simulates only the front or the rear half of the vehicle. The model has both of the front or rear wheels and the attached suspensions. The model is usually used to simulate the roll dynamics and check the vehicle stability. Usually two half car models are utilized to find about the roll characteristics of the vehicle, one for the front half and the other for the rear half, as the suspension characteristics and geometry are different for front and rear wheels.
- Four Wheel Model: Four-wheel model is the complete dynamic model of the system. It has all the wheels and suspension attached to them. Full vehicle mass is used for the

simulation of this model. This model can be used for all types of simulations and is the most accurate.

1.5 CONTRIBUTION OF THE THESIS

The contributions of the thesis are as follows:

- Eigenvalues separation method discussed in detail.
- Bond graph model of antilock braking system was developed and reduced using the Eigenvalue separation method.
- Bond graph model of bicycle model in the horizontal plane for simulation of steering was developed and reduced using the Eigenvalue separation method.
- Eigenvalue sensitivity method discussed in detail.
- Bond graph model of bicycle model in vertical plane was developed and reduced using the Eigenvalue separation method.
- Bond graph model of four wheel vehicle model was developed and reduced using the eigenvalue separation method.

1.6 ORGANIZATION OF THE THESIS

This thesis is organized in five chapters, which are introduced as follows

Chapter 1 introduces to the basics of bond graph modelling technique and its various elements. The basic concept and types of model reduction methods are also discussed. The basics types of vehicle dynamic models are introduced. The chapter concludes with the discussion on contribution and organization of the thesis.

Chapter 2 deals with the summary of the literature survey performed for the completion of the thesis. The literature review was done in three areas i.e. (i) bond graph technique and applications, (ii) various systems in automobile and dynamic analysis of these systems, and (iii) different model reduction methods. The literature gap and objectives of the present work are discussed.

Chapter 3 deals with the Eigenvalue separation method of model reduction. The chapter discussed the method, procedure and limitations of this method in detail. Two case studies relating to application of the method are also discussed.

Chapter 4 deals with the Eigenvalue sensitivity method of model reduction. The chapter discussed the method, procedure and limitations of this method in detail. Two case studies relating to application of the method are also discussed.

Chapter 5 concludes the thesis and suggests scope for future research.

CHAPTER 2 LITERATURE REVIEW

2.1 INTRODUCTION

The literature review done for the completion of the thesis and the objective of the thesis is discussed in this chapter. The literature review was done in three areas i.e. (i) bond graph technique and applications, (ii) various systems in automobile and dynamic analysis of these systems, and (iii) different model reduction methods, their advantages and limitations.

2.2 LITERATURE SURVEY

2.2.1 Literature survey on bond graph modelling technique

Bond Graph is a modelling technique by which the dynamics of a system can be represented. The technique can be used to model systems from different types of energy domains like electrical, thermal, mechanical *etc*. Bond graph technique is especially useful if the system consists of sub-systems from different energy domains. Any system can be represented by predefined elements which describe the behavior of different components in the system [**4–6**].

Mathematical modelling of a system and simulation of the system using these mathematical equations under different conditions is an important part of the design process. If the system becomes very complex, deriving the mathematical equations can become very difficult using the traditional methods. These systems can be easily handled using the bond graph technique. In this technique, bonds are drawn connecting different elements in the system and differential equations describing the system can be found by analyzing one component at a time. The process can be automated and can be programmed [**7**].

Mechatronics systems generally consist of mechanical systems and an electronic controller. Bond graph technique can be used for designing, fault estimation, identification and diagnosis in a mechatronic system. The design process of the mechatronic system consists of utilizing various tools for controller design such as drawing the signal flow graph. The bond graph technique the whole system is analyzed systematically; the signal flow graph can be drawn directly and easily from the bond graph. Hence, bond graph is a powerful tool for analyzing mechatronic systems [**3, 8–10**].(8-10)

Modelling a complex thermodynamic system, using the conventional bond graph technique is very difficult. For such systems, convection bond graphs are drawn to represent the system. In a convection bond graph, two independent effort variables were used for simulating the system, instead of one effort variable in a conventional bond graph. The two

efforts are represented by drawing a dashed line parallel to the solid line in the bond graph [**11**].

Only some specific essential information of a system is required to solve the system using bond graph technique. This information must be conveyed in such a manner, so that it can follow some algorithm to derive the differential equations describing the system. So, the main idea of the bond graph technique is to formulate some kind of language, which can convey the essential characteristics of the system, to the computer, for pre-defined algorithms to be applied on it. [**12**].

2.2.2 Literature survey on vehicle dynamics

Vehicle dynamics is the field of study of dynamics of vehicles, here considered to be four wheeled ground vehicles. The study is concerned with the performance, comfort and safety of the vehicle in motion. The major components which determine the dynamic behavior of the vehicle are, tires, suspension characteristics, suspension geometry, center of mass of the vehicle, roll axis of the vehicle, distance between center of mass and roll center, steering geometry, wheel base and track width. The systems of the vehicle are modeled in different frames of reference and then joined together to have a complete dynamic model of the vehicle [**13–15**]

Due to the friction between tyre and road surface, tire forces and moments are generated. These are crucial parameters for proper handling and safety of the vehicle. The tyre force model has two components i.e. lateral tire force and longitudinal tire force. These forces depend upon the tyre slip angle and slip ratio. The lateral forces also cause a tyre aligning moment because of the deformation of the tyre. The magic formula is an empirical expression that is used in finding the tyre forces, based on tyre slip [**16**].

A quantitative and systematic modelling and simulation technique for vehicle dynamics using bond graphs was presented [**17**]. The author also discussed the steady-state behavior and transient models for small as well as large steering input and other disturbances. Effect of various shape factors and type of characteristics on handling properties was analyzed. The quarter-car model, using one-fourth of the vehicle mass and one suspension was considered. The tire and suspension had two degrees of freedom. Bicycle model was used to include both the body bounce and body pitch. A half car model was utilized to observe and optimize the vehicle roll. Different half car models were used for front and rear half. A full car model with seven degrees of freedom was also simulated. Random vibration

analysis was performed on the models. Results showed that the base excitation frequency highly affects the vibration amplitude of the sprung mass.

Bond graph of a four wheel non-linear vehicle dynamic model was developed and simulated [**18**]. The model simulated the coupling of vertical, longitudinal and lateral dynamics of the vehicle along with the geometric non-linearity from the suspension system. The tires were modelled using Pacejka's model. Simplified engine and transmission systems were also considered. The various systems were connected through general mathematical transformations. The simulation experiments which correspond to standard vehicle dynamic tests were performed to show the vehicle performance.

Advanced automotive transmission and drive systems can also be modeled using bond graph technique [**19**]. The author modeled various systems which included one-mode as well as two-mode, series-parallel hybrid electric transmission, continuously variable transmission, torque varying and active slip differential for both two wheel drive and four wheel drive vehicles and wet and dry clutch using an electro-mechanical actuator.

The magic formula tyre can handle combined slip condition. The magic formula was tested using Carsim software and Matlab [**20**]. A vehicle was designed in Carsim and a double lane change test was performed on it at a speed of 120 km/hr. The slip angle and slip ratio were generated during maneuvering. A magic formula tyre was developed in Matlab Simulink. The slip angle and slip ratio data from Carsim was imported to Matlab as input, and the same test was performed in Matlab. Models from both the softwares were compared on lateral force, longitudinal force and aligning moment. The results had similar trend. There was a difference in magnitude due to the aerodynamic effects, gear shifting effect and kinematics of suspensions. Variation due to these factors was not modeled in Matlab.

The road interaction is one of the most important and critical parameters in the study of vehicle dynamics. A bond graph model for tyre-road interaction was developed in multi-domain [**21**]. Only one representation of complex dynamics was used, which allowed the estimation of longitudinal contact forces. The model was used in the development of a fault detection and identification algorithm for improving vehicle safety. The model described the interaction between mechanical, hydraulic, pneumatic and thermal systems. Linear velocity of vehicle and wheel was given as input to the model. The model considered a non-linear driving and braking phase. Experimental data from a Renault truck with known dynamic properties was used for analysis.

A major obstacle in implementing vehicle stability and control is the uncertainty in vehicle parameters & state and the road conditions like banking angle of the road, tire

cornering stiffness, vehicle slip angle. The vehicle slip angle and road banking angle are lumped on lateral dynamics which make it difficult to measure. New algorithms were proposed for calculation the vehicle slip angle and road banking angle [**22**]. Two algorithms were proposed, yaw-rate dynamic based approach and lateral-tyre-force-based approach. Both the algorithms utilized the known parameters of the vehicle and sensor data. The slip angle and road banking angle is then found using algebraic relations. The algorithms could also be used to estimate the cornering stiffness without knowing the road banking, by using data such as steering angle, lateral acceleration and yaw-rate. No supplementary sensors are needed for implementing the algorithm.

Another method of obtaining slip angle, tyre force and wheel cornering stiffness. The method utilized yaw-rate, longitudinal acceleration, lateral acceleration, steering angle and angular velocity of the wheel for calculation [**23**]. An adaptive tire-force model was proposed taking into consideration the variation in road friction. The process was based on two blocks in series. The first block contained a sliding-mode observer to calculate tore-road force. The second block contained extended Kalman filter to estimate side slip angle and cornering stiffness.

Antilock braking system is difficult to control due to its strong non-linear and uncertain characteristics. To overcome this, an integrated model consisting of gray system theory and sliding mode control was proposed [**24**]. Prediction capability of gray system theory and the robustness of sliding mode control was combined and used to regulate optimal wheel slip depending on the vehicle longitudinal velocity. In the calculations, a point was used as a sliding control surface instead of a line. The algorithm was tested on a quarter vehicle model. The angular velocity of the wheel and linear acceleration of the vehicle were measured and the data was used to predict if the wheel was about to lock. Four controllers, i.e. proportional-integral-derivative(PID), PID with gray predictor, sliding mode controller and sliding mode controller with gray predictor were simulated and compared. Gray predictor and sliding mode controller approach resulted in less steady state error, less overshoot and better noise reduction.

Stability and maneuverability of a vehicle is an important aspect to be considered while designing a vehicle. The chassis, suspension system, tyres and joints were modeled separately and connected to obtain the complete vehicle model. Traction was modeled as an independent parameter on the wheels, making the model applicable to electric and hybrid vehicles. By changing the direction of torque acting on the wheel, both antilock braking

system and regenerative braking were simulated. The model was able to produce simple situations in which the vehicle could become unstable and could lose maneuverability [**25**].

Vehicle testing is done in many stages of production of vehicle. The first stage is the virtual testing. This is actually a numerical simulation of the mathematical model. The limitation of virtual testing is that simulation can only be done for known circumstances and for which mathematical modelling is possible. A technique was described for using a scaled vehicle to facilitate prototyping. Concepts in the scaling process were reviewed. For a case study, a one-fifth scale vehicle test bed was presented. Antilock braking system and controller were modeled on a scaled system. It was observed that if the tyre surface interaction for scaled model is similar to the actual condition, the results describing the dynamics of the scaled system closely match the full system [**26**].

2.2.3 Literature survey on model reduction

Model reduction has been a very old concept with many mathematical techniques been introduced for the reduction process. Moment matching method [**1**] eliminated the higher order moments to reduce the mathematical calculations. The least squares method was used the technique of minimisation of the deviation of low order auto regressive moving average [**2**].The balanced truncations approach [**27**] utilised coordinate transformation to reduce the order of the transfer matrix. The worst case scenarios were used for this method.

A method of physical reduction was introduced [**28**] by observing the power flow associated with the elements in the system. The process had three steps i.e. first, system's time response the input was calculated. Second, the power flow in and out of components was measured. Third, the components associated with a low power flow were removed. The power responses were obtained by applying a step input for a given time interval and power associated with all bonds of the bond graph was calculated. Then, a root mean square (rms) average of each power was calculated. Finally, the bonds with low average values were eliminated.

Energy as a metric instead of power was preferred as energy is the time integral of power and hence more advantageous when there are time-varying elements [**29**]. The authors claimed that the root mean square power metric might also provide false information due to heavy weightage to peak responses. Hence the author defined an energy based 'element activity index', which is the ratio of the energy flowing through an element to the total energy of system. The bonds that are deemed unnecessary are eliminated from the bond graph model by removing the low activity elements to a chosen appropriate threshold value. A major

advantage of the method is that by applying a sinusoidal input the most appropriate reduced model can be obtained as a function of a frequency range of interest. An algorithm called model reduction algorithm (MORA), was also proposed on basis of activity index.

MORA was applied and tested to reduce the vehicle dynamics model of a full vehicle model [**30**]. The vehicle model consisted of engine, transmission, dynamic system and tyres. The engine model was a steady state torque map obtained from the thermodynamic data of a real engine. The transmission consisted of a torque converter, transmission and driveline. The longitudinal, heave and pitch motion of the system were found by using a non- linear model. The model was configured for a class VI truck and simulated in 20 SIM environment. Energy based MORA algorithm was applied to reduce the model. In the algorithm, an energy metric was found for all the elements, and was compared. The reduction resulted in removal of 37 out of 55 elements in the reduced model. The truck was simulated from standstill and accelerated to 60 MPH. The speed profile predicted was highly accurate.

On similar lines of 'element activity index' as discussed previously, a junction inactivity index was measured to find a simplified model [**31**]. A junction was assumed inactive if there was very little flow in a 1-junction or if there was very little effort in a 0-junction. A hypothesis was presented that an inactive junction structure could be removed without affecting the accuracy of the model but, removing of junction did not necessarily correspond to removal of all the null powered bonds.

Singular perturbation theory is used to dissociate mathematical equations into two time scales. A similar approach was be used on a bond graph model of the system for partitioning the system into subsystems which were dominant in different time scales. Both analytical and geometrical methods were proposed to apply the fast-slow dissociation to the to a state space model. The fast system was obtained by comparing the relative magnitudes of the elements and observing the causal connectivity between elements. The slow bond graph was obtained by first finding the reciprocal bond graph of the system. Then, the slow bond graph was found by inverting the fast system of the reciprocal bond graph [**32**].

Another method for partition of system into subsystems is was proposed based on distribution of the Eigenvalues [**33**]. The relative position of Eigenvalue because of energy interaction between the elements was found by observing the loop gains of the various causal loops and local damping ratios. Depending upon the relative distribution of the Eigenvalues, the systems could be dissociated into fast-slow subsystems, high-low frequency subsystems, highly-lowly damped subsystems. The reduced system was obtained by combining various subsystems of the same time scale. The technique was applied and verified by reducing a

seventh order single input single output (SISO) system, a tenth order SISO system and a multi input multi output system (MIMO). The details about the technique are discussed in chapter 3.

Another technique for finding a physical reduced model was given by observing the sensitivity of the Eigenvalues of the linear time-invariant (LTI) system, with respect to the various elements in the system [**34**]. A high sensitivity indicated high dependence of the Eigenvalue on that element. The elements for which the Eigenvalues sensitivity is low for all the Eigenvalues was low indicated very little importance of that element, hence was removed. The dynamics of the reduced system closely matched those of the full system. The technique is discussed in detail in Chapter 4.

2.3 LITERATURE GAP

After extensive literature survey, relating to bond graph modelling, vehicle dynamics and model order reduction, it is observed that many different types of vehicle dynamic systems have been successfully simulated using the bond graph approach. Mathematical model reduction procedures have been applied extensively in the past to reduce the effort for calculation. But very less study has been done to remove the physical components from the analysis, to reduce the calculation. The activation index method by the use of MORA, has successfully led a reduced model. But very less work has been done to reduce the model using the methods based on the Eigenvalues. So, there is a need to reduce the vehicle dynamic models using Eigenvalue based techniques as these techniques are mathematically proven and have a strong physical interpretation.

2.4 OBJECTIVE OF THE PRESENT WORK

It is observed from the literature survey that the bond graph technique is very useful in modelling various multi-body systems. The physical reduction procedures were analysed. Though the power and energy methods had very successful implementation and a very strong physical interpretation, but the technique has no mathematical basis. Hence, for this thesis Eigenvalue methods are used. The objectives of the thesis are as follows:

- Bond graph modelling and reduction of antilock braking system.
- Bond graph modelling and reduction of bicycle model in horizontal plane.
- Bond graph modelling and reduction of bicycle model in vertical plane.
- Bond graph modelling and reduction of four wheel vehicle dynamic model.

*add steering model

CHAPTER 3 EIGENVALUE SEPARATION METHOD

The Eigenvalues are of great importance in dynamics. The Eigenvalues are actually the roots of the characteristic equation of dynamic system; hence, Eigenvalues contain all the information about the behaviour of the system. These Eigenvalues set of the system can be dissociated into two or more sets giving different subsystems and having different behaviour.

3.1 METHOD

3.1.1 Introduction

The Eigenvalue separation method is based on the comparison of energy exchange rates between two different elements. This rate of energy exchange is given by the loop gain of the causal loop containing these elements. The elements which have very high exchange rates contribute to the faster subsystem. The subsystem which is obtained when the components of faster subsystem are removed and replaced with a zero source of flow element is the slower subsystem. Hence, components that occur in loops having higher loop-gain are part of the faster subsystem and those which remain after eliminating faster subsystem are part of the slower subsystem. This technique is based on the singular perturbation theory. Singular perturbation theory is used to decompose a dynamic system into two time scales i.e. fast scale and slow scale. The state-space equation without input is given by

$$\dot{x} = Ax = \begin{pmatrix} \dot{x}_1 \\ \varepsilon \dot{x}_2 \end{pmatrix} = \begin{bmatrix} A_{11} & A_{12} \\ A_{21} & A_{22} \end{bmatrix} \begin{pmatrix} x_1 \\ x_2 \end{pmatrix}, \quad \varepsilon << 1 \tag{3.1}$$

Where x_1 is state vector of slow dynamics, x_2 is the state vector of fast dynamics and ε is the normalizing factor. As the slow dynamic equations are nearly static for fast time scale point of view, the fast dynamics can be represented as

$$\varepsilon \dot{x} = A_{22} x_2 \tag{3.2}$$

Since, the fast dynamics evolve very fast, the slow dynamics evolve under the conditions that the fast dynamics have already been dissipated. Hence, the slow dynamics can be represented as

$$x_1 = \left[A_{11} - A_{12} A_{22}^{-1} A_{21} \right] x_1 \tag{3.3}$$

Figure 3.1 shows a case in which separation of Eigenvalues is possible. This is a case of fast and slow dissociation which is explained in detail in the next subsection.

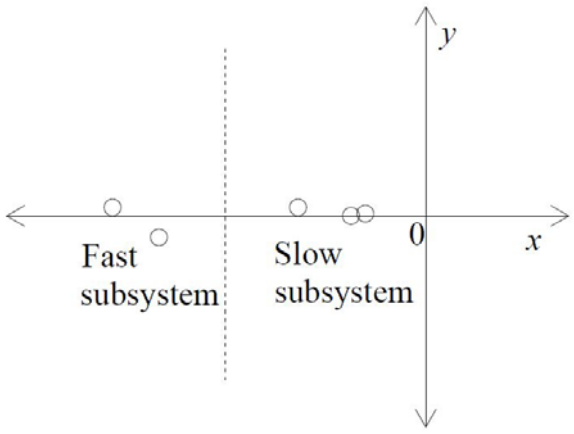

Fig 3.1 Eigenvalue distribution for fast-slow dissociation

3.1.2 Fast-slow decomposition

For purely real Eigenvalues, there is no oscillation. The behaviour of the system will be a combination of all the Eigenvalues. The Eigenvalues for the stable system are negative. So, if the magnitude of the Eigenvalue is high (i.e. Eigenvalue is more negative), the component of that Eigenvalue dissipates fast and if the magnitude of the Eigenvalue is low, the component dissipates very slowly. So, when it is required to find the state of the system after a small time scale after the start, we just need to study the fast components of the system. Minor adjustments can be made so as to reduce the error. On the similar lines, if the dynamics of the system after significant amount of time from the start is required to know, the study of the behaviour of the slow dynamic system is required as the fast components are reduced to nearly zero by that time. Figure 3.2(a) shows one such case. In this case, there are two Eigenvalues at -0.5 and -5. For this case, the slow system will have only one Eigenvalue at -0.5 and the fast system will have only one Eigenvalue at -5. The final solutions are given by the Eq. (3.4–3.6).

$$y_{\text{net}} = e^{-0.5t} + e^{-5t} \tag{3.4}$$

$$y_{\text{slow}} = e^{-0.5t} \tag{3.5}$$

$$y_{\text{fast}} = e^{-5t} \tag{3.6}$$

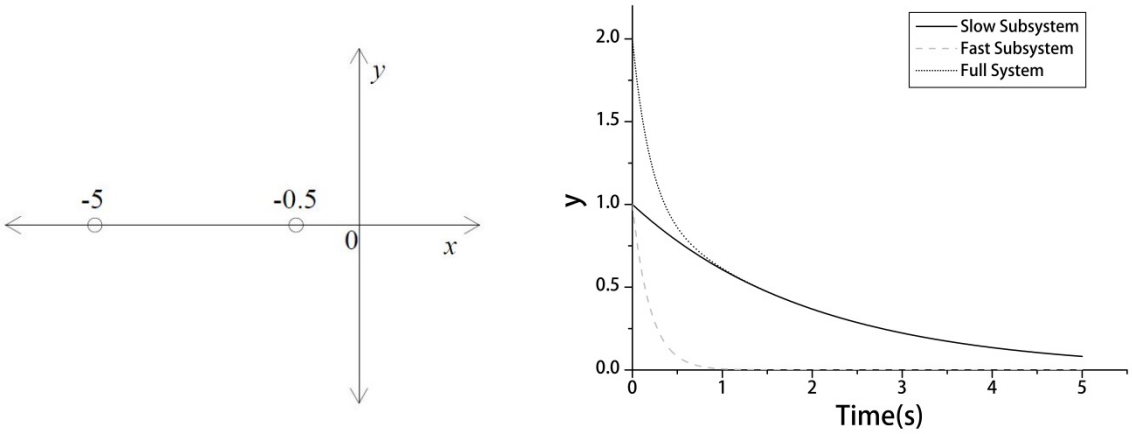

(a) (b)

Fig. 3.2 Example of fast and slow dissociation

Figure 3.2(b) shows the variation in the final output for the slow, fast and combined system with respect to time. In this case, for time 0s to 0.5s, the dynamic behaviour of the fast system and the actual system are similar. The real behaviour can be achieved form the fast system by using a scaling factor. After 0.5s, the slow system gives nearly the same behaviour as the actual system and can be used directly for simulation.

3.1.3 High-low frequency decomposition

For purely imaginary Eigenvalues, the singular perturbation theory is not applicable. The approach in such a case would be to transform the system Eigenvalues from the imaginary axis to the real axis and then the singular perturbation theory may be applied. In this case, the decomposition gives high and low frequency subsystems instead of fast and slow dynamic systems. If the roots of the system equation lie on the imaginary axis, there is no dissipation of power. So, the energy exchange is possible only between the energy storage elements i.e. I and C elements.

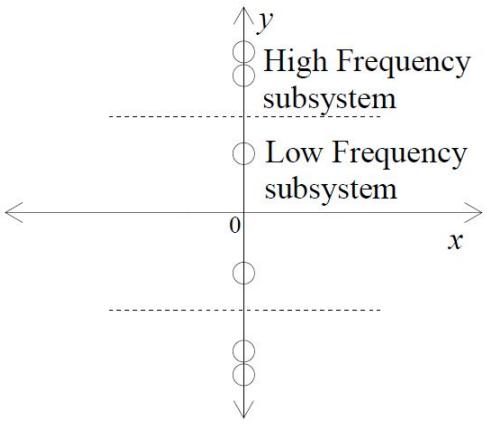

Fig. 3.3 Eigenvalue separation in high-low frequency dissociation

The system containing energy storage elements i.e. I-C system can be represented as

$$\begin{pmatrix} \dot{e} \\ \dot{f} \end{pmatrix} = \begin{bmatrix} 0 & C \\ I & 0 \end{bmatrix} \begin{pmatrix} e \\ f \end{pmatrix} \tag{3.7}$$

Where *e* is the state vector representing the efforts associated with the C elements, f is the state vector representing flow associated with I elements, C is a sub matrix containing the parameters of C elements, and I is a sub matrix containing the parameters of I elements.

$$\ddot{e} = CIe \text{ or } \ddot{f} = ICf \tag{3.8}$$

If all the I elements are replaced with R elements of the same value, the state equation reduces to

$$\begin{pmatrix} \dot{e} \\ f \end{pmatrix} = \begin{bmatrix} 0 & C \\ R & 0 \end{bmatrix} \begin{pmatrix} e \\ f \end{pmatrix} \tag{3.9}$$

Hence,

$$\ddot{e} = eCR \tag{3.10}$$

Similarly, if all the I elements are replaced with R elements of the same value, the state equation reduces to

$$\begin{pmatrix} e \\ \dot{f} \end{pmatrix} = \begin{bmatrix} 0 & R \\ I & 0 \end{bmatrix} \begin{pmatrix} e \\ f \end{pmatrix} \tag{3.11}$$

Hence,

$$\ddot{f} = IRf \tag{3.12}$$

All C-R (or I-R) systems can be decoupled like fast and slow systems giving us high and low frequency systems. The transformation brings the Eigenvalues from the imaginary axis to the real axis with two to one mapping. No need to actually replace the C or I elements with R elements in practice is required, as the mapping is always possible. The procedure of the previous case is applicable directly on the I-C systems. Figure 3.4 shows the schematic diagram of how Eigenvalues of an I-C system, which has purely imaginary Eigenvalues $(\sigma_1, -\sigma_1, \sigma_2, -\sigma_2, \sigma_3, -\sigma_3)$ can be mapped onto the real axis $(\sigma_1', \sigma_2', \sigma_3')$.

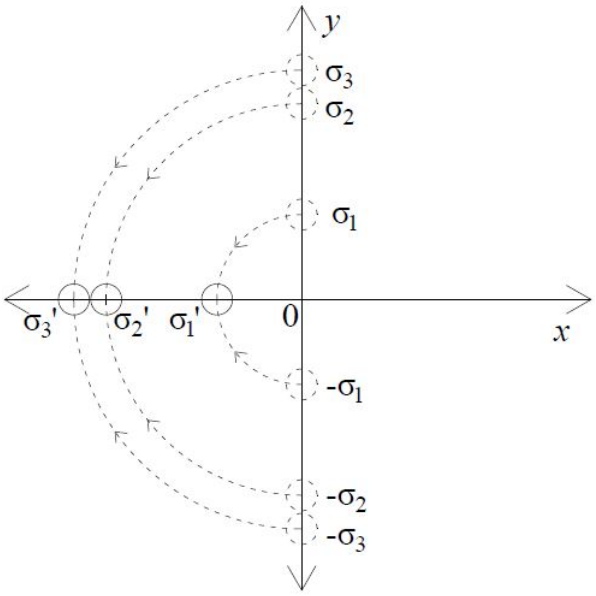

Fig. 3.4 Mapping of I-C system into I-R system

3.1.4 High-low damped decomposition

In the previous subsections the cases in which Eigenvalues are purely real or purely imaginary i.e. systems with very high damping or very low damping were discussed. The former consists of only I-R or I–C element loops while the latter consists of only I–C loops. But in most real life problems, I, C and R elements may be present. To deal with such a case, the local damping ratio between the components is required to be calculated. If all the local damping rations are very small, the Eigenvalues must be nearer to the imaginary axis; so, the system can be treated as I–C system and decoupling can be done to find the high and low frequency subsystems. Similarly, if all the local damping ratios are very high, the system must have Eigenvalues close to the real axis. In this case the system can be decomposed into fast and slow dynamic components. But if in a system some of the local damping ratios are high while the others are very low, the system has some Eigenvalues close to real axis and some Eigenvalues close to the imaginary axis. Such a system must first be divided into heavily damped subsystem and lowly damped subsystem. Heavily damped subsystems can be further decoupled into fast and slow subsystems while the lowly damped subsystem can be subdivided into high and low frequency dynamics. The Eigenvalue distribution for which high and low damped dissociation is possible is shown in Fig. 3.5.

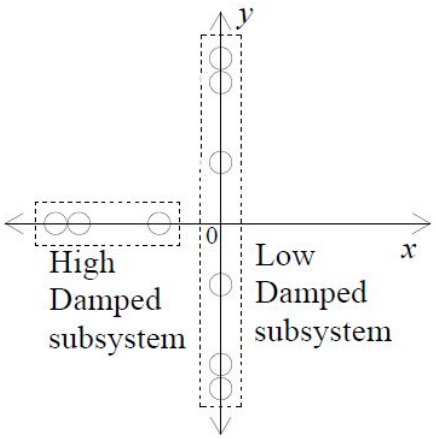

Fig. 3.5 Eigenvalue distribution for high-low damped system dissociation

3.2 PROCEDURE

First, the local damping ratios of the system are found. If all the local damping rations are very small, all the Eigenvalues can be considered as purely imaginary. The system can be treated as I–C system and decoupling can be done to find the high and low frequency subsystems. Similarly, if all the local damping ratios are very high, the system can be divided into fast and slow dynamic components because for such a system, the Eigenvalues can be considered to be purely real. But if in a system some of the local damping ratios are high while the others are very low, the system must first be divided into heavily damped subsystem and lowly damped subsystem. Heavily damped subsystems can be decoupled into fast and slow subsystems while the lowly damped subsystem can be further subdivided into high and low frequency dynamics. Figure 3.6 shows the flow chart of the generalized procedure.

3.2.1 High and low damped decomposition

For high and low damped decomposition, in addition to the loop gains for each energy storage element, the local damping ratios should also be calculated. For each directly causally related I–C pair in the system (with R-elements causally connected to I or C or both elements), the local damping ratios can be calculated as $G_{RC}/2\sqrt{G_{IC}}$ and $G_{RI}/2\sqrt{G_{IC}}$ for the C and I elements, respectively. In these formulae, G_{IC} represents the I–C loop gain, G_{RC} represents the sum of the loop gains of R–C pairs and G_{IR} represents the sum of the loop gains of I–R pairs. This gives the damping ratios of the system.

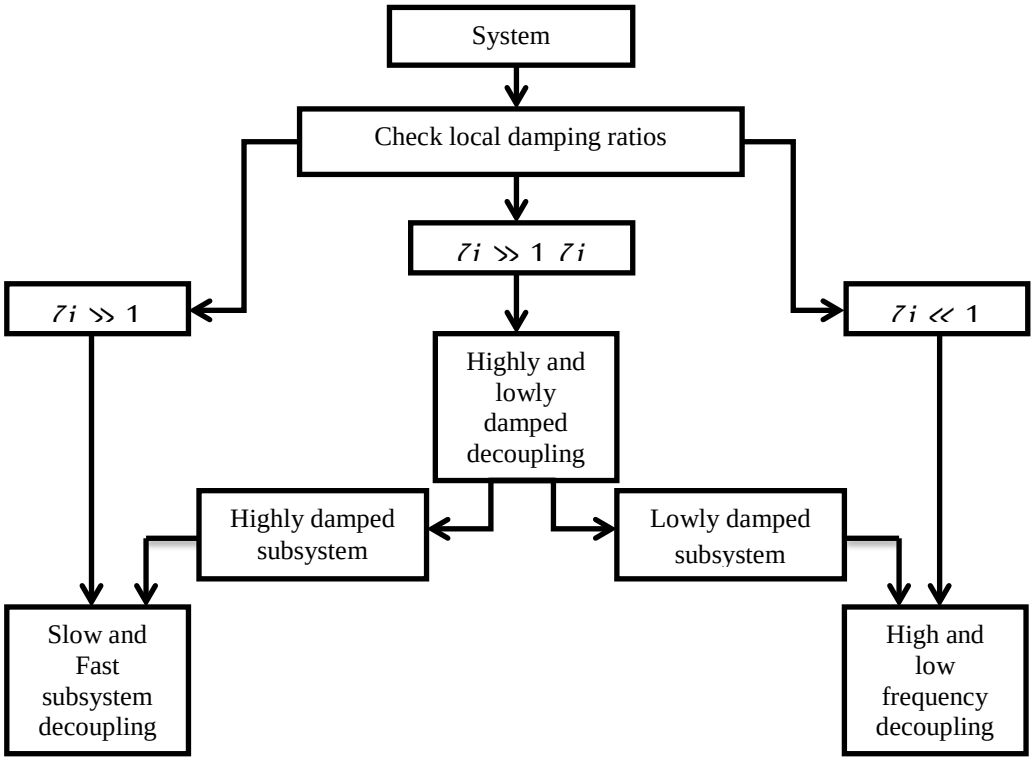

Fig. 3.6 Generalized Procedure for Eigenvalue separation method

Identification of heavily damped subsystems

1. All the C elements are replaced by flow sources of zero value. The remaining R-I pairs, causally related directly are identified. These R-I elements and the involved junctions are added to a set called H.
2. C elements are restored. The C elements, which are causally related to the above I elements are identified. If $\sqrt{G_{IC}} >> G_{RI}$, the C elements are replaced by flow sources with zero value. These flow sources are added to the subsystem H.
3. I elements that become dependent because of the causalities imposed by the above flow sources are identified and denoted in subsystem H.
4. The above procedure is repeated for I elements. In this case effort sources are used instead of flow sources.
5. The resistances, involved in the heavily damped local loops, are identified. These R elements along with the involved I–C pairs and junctions are added to subsystem H.
6. The C elements not involved above step, but causally related directly to I elements discussed above are identified. If $\sqrt{G_{IC}} >> G_{RI}$, replace the C elements by flow sources of zero value. These flow sources are added to subsystem H. In case of opposite inequality, the C element is ignored.

7. Step 6 is repeated for I element. For the step flow source in step 6 is replaced by effort source.
8. Remove the elements not in H. This gives heavily damped system.

In the procedure, step 1 identifies I and R elements responsible for heavily damped modes, given that they affect the dynamics even if all of the capacitances are disabled. Steps 2 and 3 identify I-elements involved in the heavily damped modes by the power transmission through I–C loops. Steps 4 repeat the same procedure for R-C elements. Step 5 includes the over damped subsystems. Steps 6 and 7 identify I or C elements that affect the heavily damped modes by power transmission through other I–C loops.

Identification of lowly damped subsystems

1. I–C pairs involved in lightly damped local loops are identified. These I-C elements are denoted as part of a set called L.
2. R-elements not involved in step 1, but are causally related to the above I or C elements, are identified. If $\sqrt{G_{\mathrm{IC}}} << G_{\mathrm{RI}}$, the resistive R-elements are replaced by flow sources with zero value and the conductive R-elements are replaced by effort sources with zero value. These sources are denoted as part of the subsystem L.
3. I or C elements that become dependent, because of the causalities imposed by the sources are identified and denoted as part of subsystem L
4. Remove the elements that are not denoted as part of the subsystem L.

3.3 LIMITATIONS

As the bases of dissociation in the said method are ratios and loop gains, the approximate distribution of Eigenvalues is known and not the real Eigenvalues themselves. This also leads to some limitations.

- The first limitation is that it creates a blind spot for Eigenvalue which is not nearer to any of the axis. This situation is indicated by local damping ratios close to 1. Subsystems contributing to these Eigenvalues cannot be dealt with using this method.
- Secondly, sometimes Eigenvalues may affect a system due to its absolute position but may be neglected in by the method, as this method is based only on comparison with other Eigenvalues.

- The third limitation of the model is that there is no definite method of distinction between time frame of faster and slower subsystem. A time frame for faster calculations in one model may be the time frame for slower calculations in the other model.

Figure 3.7 summarizes the various regions of different types of dissociations and the region in which the dissociation using the Eigenvalue separation method is not valid.

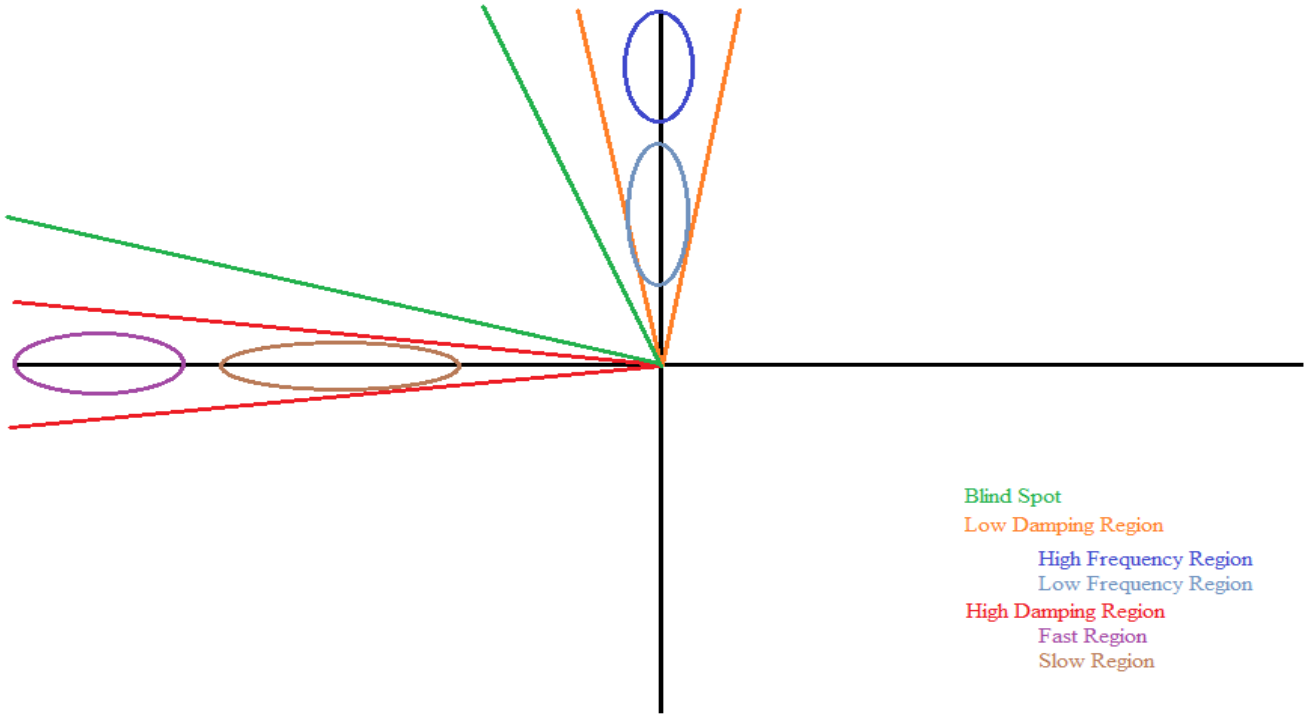

Fig. 3.7 Working region of various Eigenvalue separation methods

3.4 CASE STUDY I: ANTILOCK BRAKING SYSTEM

3.4.1 Bond graph model of antilock braking system

Antilock braking system (ABS) is used in automobiles for an improved performance and better control over the vehicle for different road scenarios. The objective of ABS is to maintain an optimal slip ratio. The mechanical equivalent of ABS model shown in Fig. 3.8 is used for simulation.

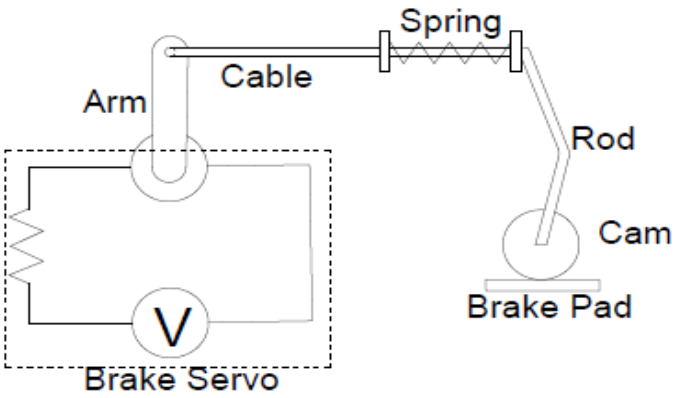

Fig. 3.8 Schematic diagram of ABS [**35**]

The braking signal is actuated by the driver by pushing the brake pedal. At this point the various sensors placed on the vehicle to provide longitudinal speed of the vehicle and angular speed of the wheels. By comparing these quantities, the slip ratio can be found out. Slip ratio during acceleration and braking is given by

$$\text{Slip ratio (during braking)} = \frac{\dot{x}_w - \dot{\theta}_w r}{\dot{x}_w} \tag{3.13}$$

$$\text{Slip ratio (during acceleration)} = \frac{\dot{\theta}_w r - \dot{x}_w}{\dot{\theta}_w r} \tag{3.14}$$

Initially, the angular speed of wheel decreases before there is a decrease in the longitudinal speed of vehicle when brakes are applied. This increases the slip ratio. At high value of slip ratio, the grip between road and tire decreases; so, when the slip ratio reaches a predefined maximum value, the braking torque is released. Similar to conditions of high slip ratio, a low slip ratio also decreases the grip between road and tire. So, if slip ratio drops to a predefined minimum, the braking torque on the wheel is increased. The operating logic is summarised in Fig. 3.9.

The traction acting on the tyre may be presented by *Pacejka's magic formula*, which defines the longitudinal force, lateral force and self-aligning moment as a function of longitudinal slip and side-slip, respectively. This function is given by

$$y_0 = D\sin[C\tan^{-1}\{B x_i - E(B x_i - \tan^{-1}(B x_i))\}] \tag{3.15}$$

Where the output variable y_o can be F_x, F_y or M_z and the input variable x_i can be $_x$ or σ_y. The constants *B, C, D* and *E* are determined from experiments.

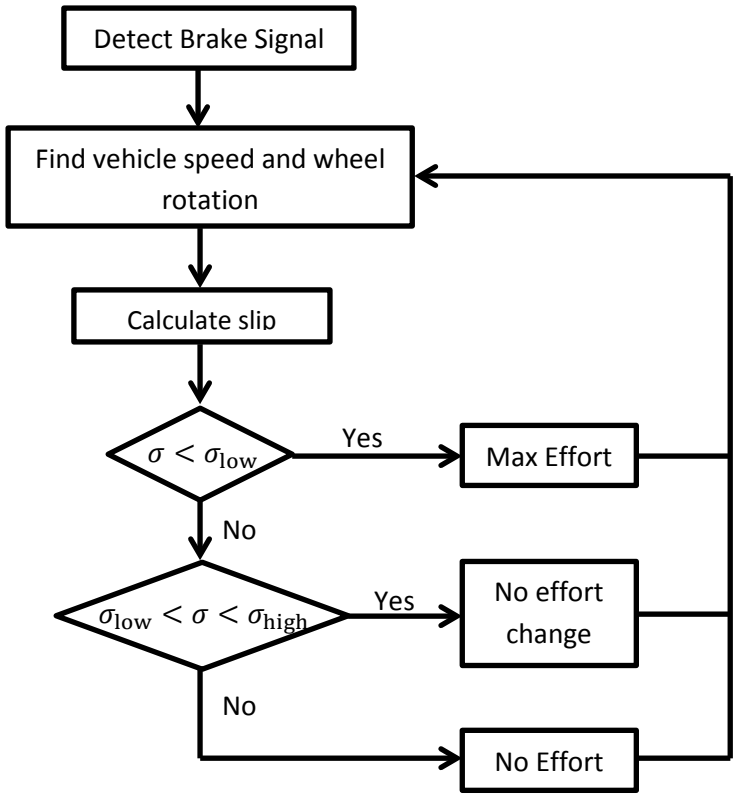

Fig. 3.9 Operating logic of ABS [**35**]

Figure 3.10 shows the bond graph of ABS system. The torque obtained from the motor is shown as Se-element. The rod magnifies the motion of the shaft and hence is shown by a transformer element. The losses at the end of the rod are shown by R-element. The stiffness of the cable connected at the end of the rod is modeled by C-element. The other end of the cable is attached to a spring shown in the bond graph with another C-element. As this spring is fixed at one end, a flow source of zero value is connected to it. The flow at the end of the cable is transferred to the wheel through a rod. The moment of inertia of the wheel is represented by I-element and the flow transformation due to rod is expressed with a transformer element.

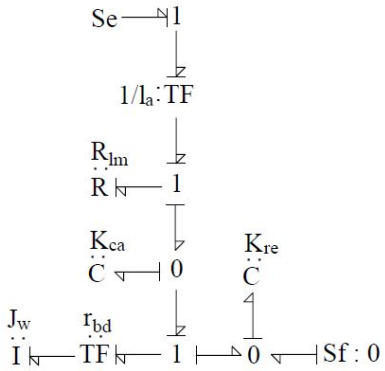

Fig. 3.10 Bond graph of ABS [**35**]

3.4.2 Eigenvalue separation technique

For ABS (Fig. 3.10) there are three causal loops given in Table 3.1. In the system there is only one local damping ratio $\left(G_{L1}/2\sqrt{G_{L2}}\right)$ which is much greater than 1. So, the subsystem is assumed to be highly damped and dissociation is done for fast and slow subsystems. R_{lm} and K_{ca} are the elements associated with loop with high loop gain. These form the major components in the fast subsystem. But, it is observed that the fast subsystem does not contain the component of interest i.e. wheel. Hence, we also find the slow subsystem.

Table 3.1 Causal loops in ABS bond graph model

Loop no.	Loop	Loop type	Loop gain (G)
L_1	R_{lm}-K_{ca}	RC	25000
L_2	J_w-K_{ca}	IC	15
L_3	J_w-K_{re}	IC	1500

3.4.3 Reduced Model

Slow subsystem is shown in Fig. 3.11. The physical interpretation is that the exchange of energy between R_{lm} and K_{ca} is too high and dissipates before any observable effect, hence slow system can be used as approximation for all times. It is to be noted that for the slow subsystem, the C-element has a differential causality. Hence, a boundary condition is provided for solving the system i.e. rate of change of spring stiffness is zero.

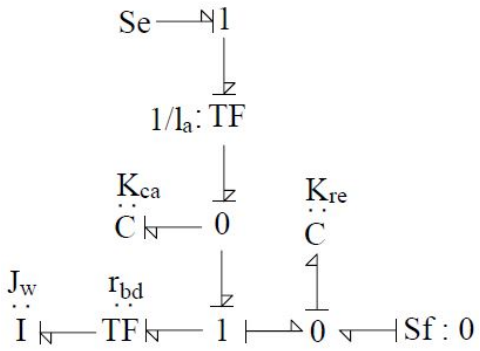

Fig. 3.11 Reduced bond graph model of ABS

3.4.4 Parameter values and simulation results

The ABS model is simulated to operate at voltage to produce a braking torque of 100 Nm, and is connected to a wheel having a moment of inertia of 15 kg m^2. Arm length l_a = 1m, R_{lm} = 0.04 Ns/m, K_{ca} = 10^4 N/m, K_{re} = 10^6 N/m and the wheel has a radius of 0.15 m.

The full system and reduced system were compared by observing the torque to the wheel. The difference between results of the models was plotted and is shown in Fig. 3.12. The reduced system gives very close results as compared to the full system.

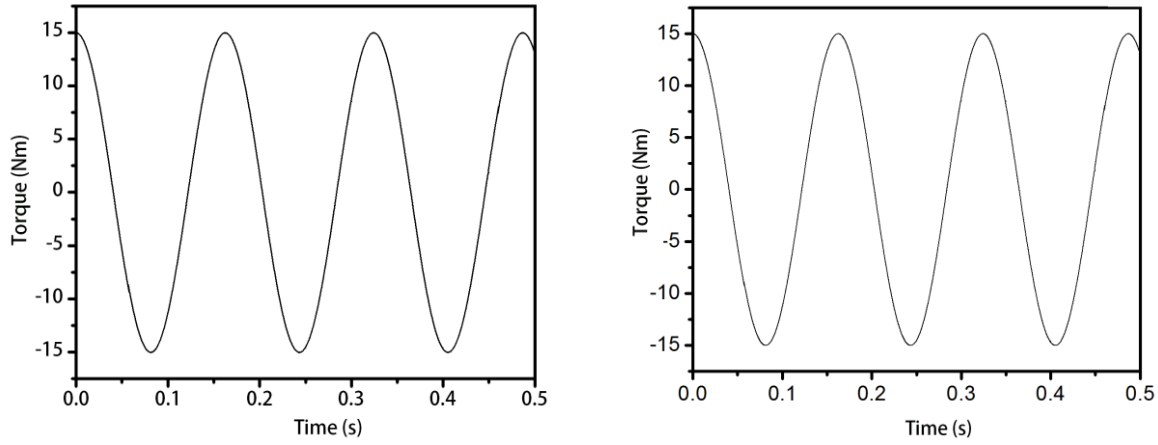

(a) (b)

Fig. 3.12 Comparison of torque observed at wheel for (a) full model and (b) reduced model

Figure 3.12 shows the comparison of braking torque achieved for the full and reduced ABS models. The results are very close and can be considered within the error limits of computation. But from the Fig. 3.13(b), it is noted that the percentage error of the system follows a cyclic variation, and reaches very high values, but such an error is not observed when comparing the torque directly. The error percentage increases at times when the torque on the wheels is close to zero. So, a percentage error compared to such a small base term may give a high percentage of error, even if the error is within acceptable limits in absolute terms. This can be observed from Fig. 3.13(a), which shows the absolute error in torque observed at the wheel between full and reduced model.

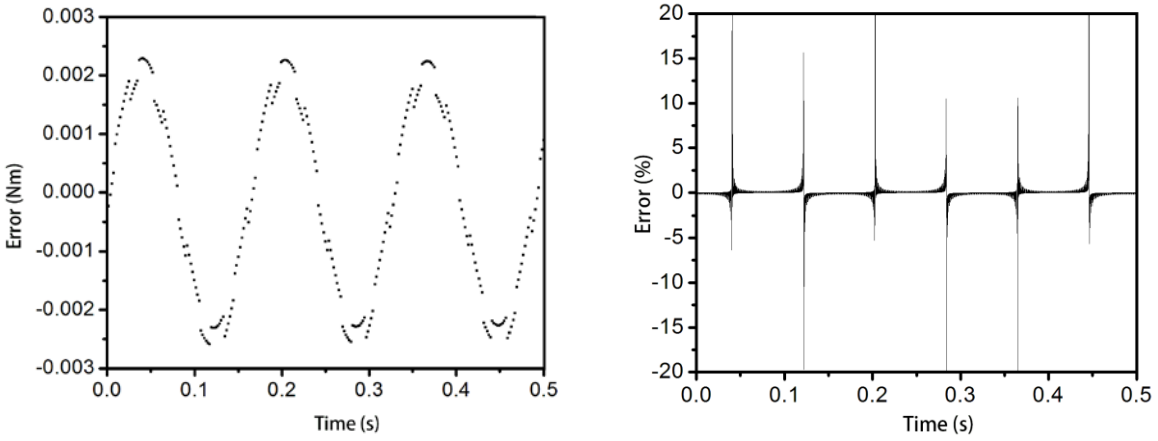

(a) (b)

Fig. 3.13 (a) Absolute and (b) Percentage error between torques for full and reduced model

3.5 CASE STUDY II: STEERING IN BICYCLE VEHICLE MODEL

Bicycle model, is an approximation of a four wheel vehicle under the assumption that there is no lateral load transfer.

3.5.1 Bond graph of bicycle model with steering

The bicycle model used here, lies in the horizontal plane and does not consider the pitch, roll and heave motions of the vehicle. The dynamics due to suspensions are also neglected. These assumptions do not allow any kind of lateral load transfer in the vehicle during the maneuvering.

Figure 3.14 (a) shows the schematic diagram of the model and Fig. 3.14 (b) shows the word bond graph of the model. CTF in word bond graph represents the necessary coordinate transformation. Kinematic equations used for creating the bond graph are as follows

$$v_{\text{nfr}} = \left(\dot{y} + \dot{\theta}_{\text{cz}}\, a\right)\cos d - \dot{x}\sin d \tag{3.16}$$

$$v_{\text{tfr}} = \left(\dot{y} + \dot{\theta}_{\text{cz}}\, a\right)\sin d + \dot{x}\cos d \tag{3.17}$$

$$v_{\text{nrr}} = \left(\dot{y} - \dot{\theta}_{\text{cz}}\, b\right) \tag{3.18}$$

$$v_{\text{trr}} = \dot{x} \tag{3.19}$$

As the model is in the horizontal plane, one translation and two rotational constraints are added. Hence, the Newton-Euler equations are reduced to

$$m_{\text{v}}\,\ddot{x} = m_{\text{v}}\,\dot{\theta}_{\text{cz}}\,\dot{y} + \sum F_{\text{X}} \tag{3.20}$$

$$m_{\text{v}}\,\ddot{y} = -m_{\text{v}}\,\dot{\theta}_{\text{cz}}\,\dot{x} + \sum F_{\text{Y}} \tag{3.21}$$

Figure 3.15 shows the bond graph model of the system. The system runs using a motor, in which the input voltage is shown as an effort source. Due to the resistance in the motor, using ohm's law we get the magnitude of current in the motor. The gyrator provides the torque generated in the motor. This torque is scaled using a transformer element which represents the gear ratio. The final torque is fed to the rear wheel. I-element i.e. the moment of inertia of the wheel takes up effort (torque) from the system and returns flow (angular velocity). The rolling resistance in the wheel is shown by an R-element. The angular speed of wheel is converted into linear speed of vehicle using a transformer with coefficient equal to the radius of the wheel. The linear speed is directly applied to the vehicle body. The pseudo-

forces on the vehicle body are modeled using the modified Newton-Euler equations given in Eq. 3.20 and 3.21. Newton-Euler equations are implemented by placing a gyrator element between the horizontal and lateral velocity of the vehicle.

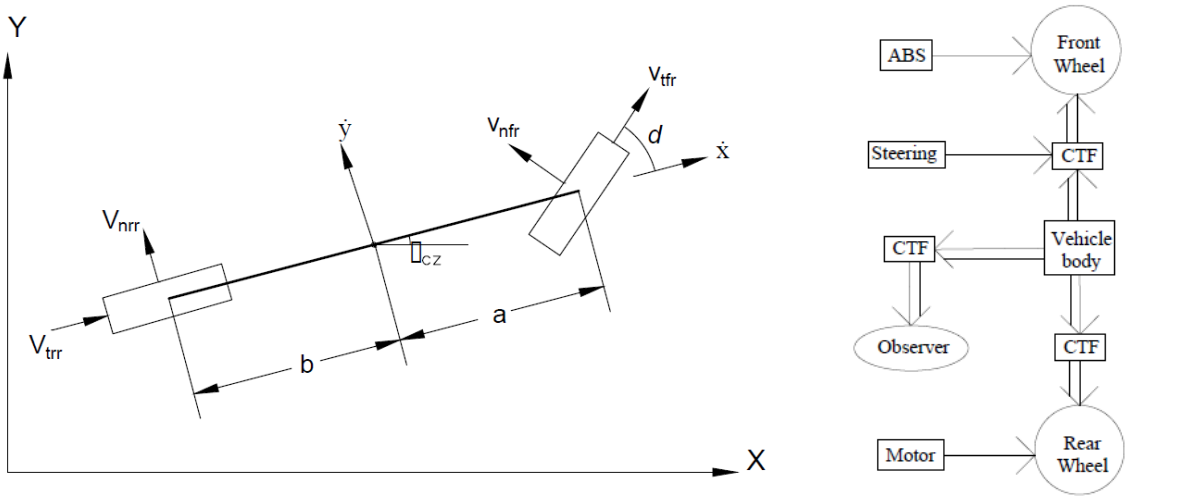

(a) (b)

Fig. 3.14 (a) Word bond graph (b) Schematic diagram of bicycle model with steering

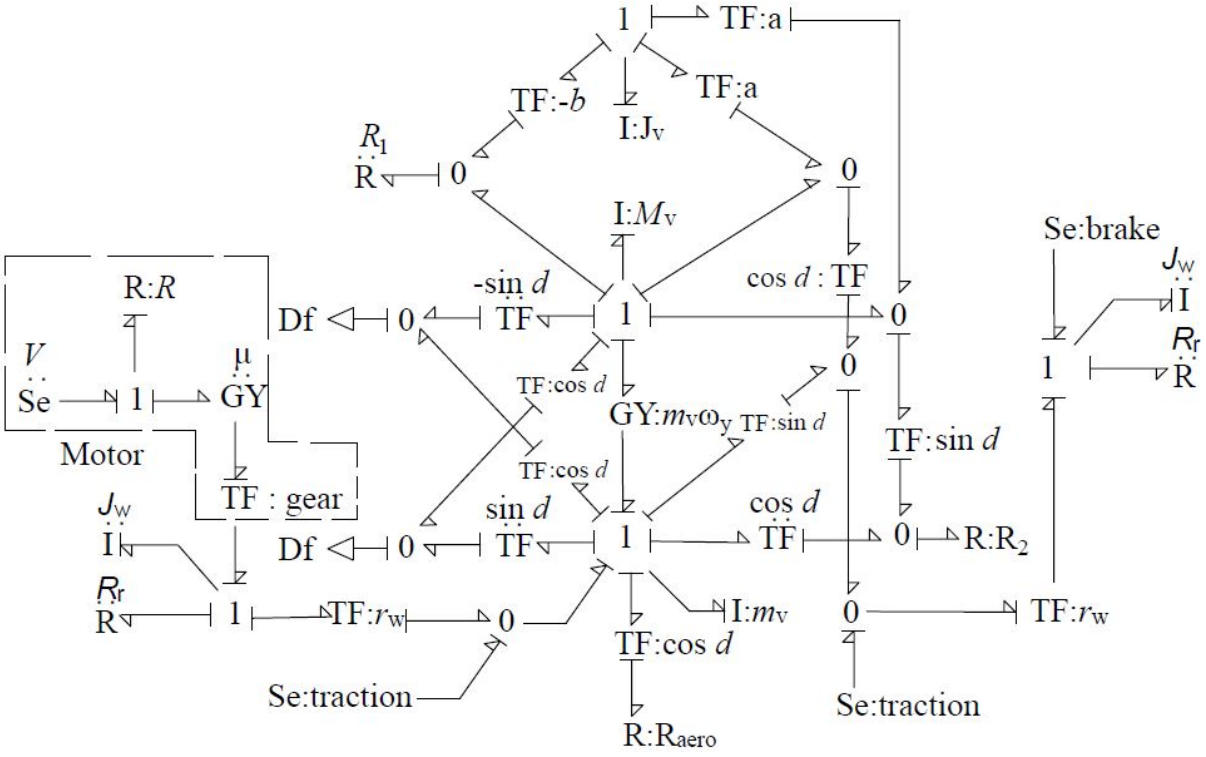

Fig. 3.15 Bond graph of bicycle model

3.5.2 Eigenvalue separation technique in steering system

The first step of the procedure is to find the local damping ratios. But, as there are no C-elements, it is not possible. Hence, the system is directly dissociated into fast and slow subsystems.

The loop gain analysis shows nine causal loops in the system as given in Table 3.2. This is a non-linear system and the loop gains of many loops are not constant with respect to time. Loops 5-9 have loop gains only when the vehicle steers by applying some steering angle *d*. The magnitude of loop gain also changes as the steering angle gradually increases. Hence, for any situation where there is no steering, these loops can be neglected.

Table 3.2 Causal loops in bicycle model without steering

Loop No.	Loop Type	Loop	Loop Gain
1	I-R	J_w-R_r (front)	382.55
2	I-R	J_w-R_r (rear)	382.55
3	I-R	J_w-R	1.024
4	I-R	m_{vx}-R_2	0
5	I-R	m_{xy}-R_1	0
6	I-R	m_{vy}-R_2	0
7	I-R	J_{cy}-R_1	0
8	I-R	J_{cy}-R_2	0

3.5.3 Reduced model

Eigenvalue separation technique cannot be applied for non-linear models; therefore, a reduced model can be obtained only for case in which the system behaviour is linear i.e. when there is no steering. The loops L_1 and L_3 can be neglected as the loop gain is very low. These loop gains add to the fast subsystem. For obtaining the slow subsystem, the elements with these loops are neglected. The parameters which take part in only these loops are R_1 and R_2. So, these can be neglected for analysis where brake force is not applied. The bond graph of the reduced model is shown in Fig. 3.17.

After a straight line path of ten seconds, the model was steered for two seconds with a steering angle of 0.1 rad. For steering, the magnitude of loop gains for loop 4–8 keeps on changing. So, the magnitudes of loop gains were compared for the duration of steering. The duration of steering was divided into various periods during which, various elements were

removed,, depending on the relative magnitudes of the loop gains. It was assumed that the loop gain could be neglected if the relative magnitude was less than 0.15. Figure 3.18 shows the variation in the relative magnitudes of various causal loops for time of 10–12 seconds, for which the vehicle was steered. For stability of the model, brake force was also applied on the wheels during steering to check reduce wheel slip.

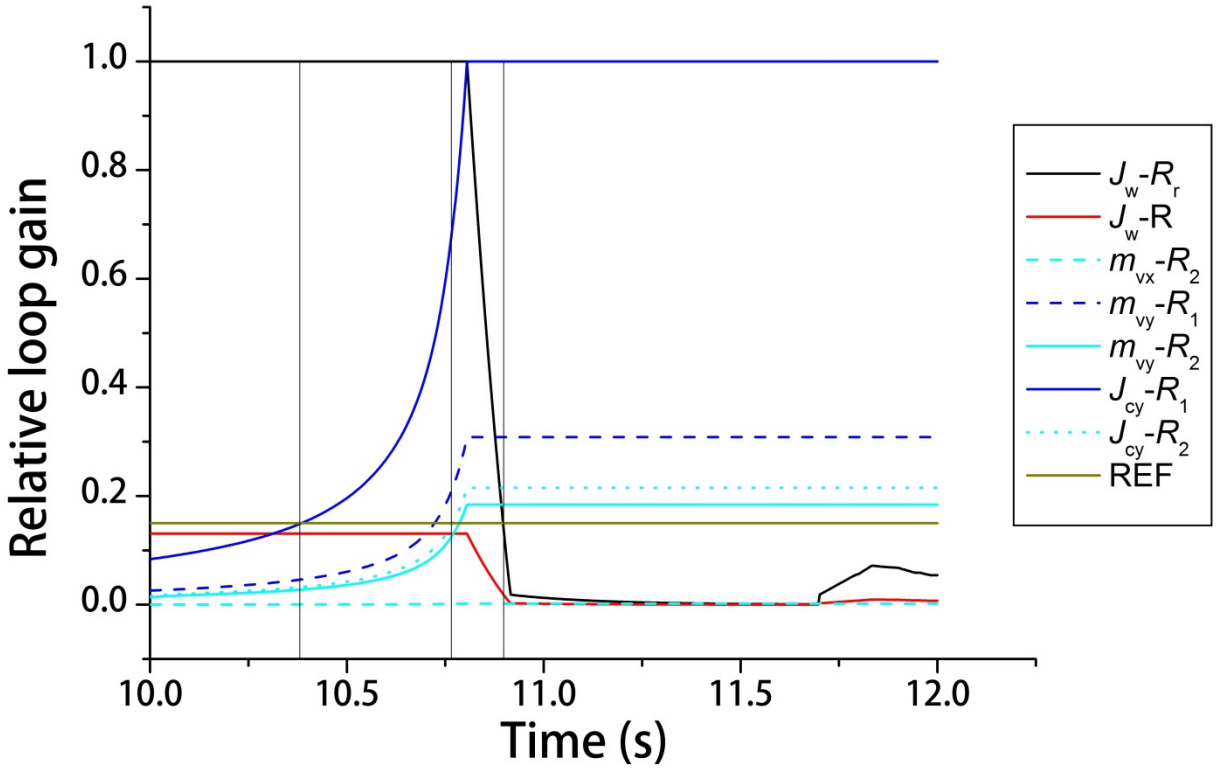

Fig 3.16 Variation of relative magnitudes of causal loops during steering

Figure 3.16 shows the variation in relative magnitudes of the loop gains. From the figure it is concluded that the steering duration can be sub-divided into four parts. The first sub-duration was from 10-10.4 sec. During this period the relative magnitudes of loops 4–8 increased continuously but were below 0.15 hence, same model was simulated. From 10.4–10.7 sec, relative magnitude of loop containing element *R*1, increased above the threshold of 0.15 so the element *R*1 was included in the model. For 10.7–10.9 sec, the loops containing *R*2, also increased above 0.15 in terms of relative magnitude. For this period full system was simulated. For 10.9–12 sec, the magnitudes of loops containing *R*1 and *R*2, became very high, due to which the relative magnitude of loops 1 and 2 dropped. So, for this period, rolling resistance (R_r) for both wheels was neglected.

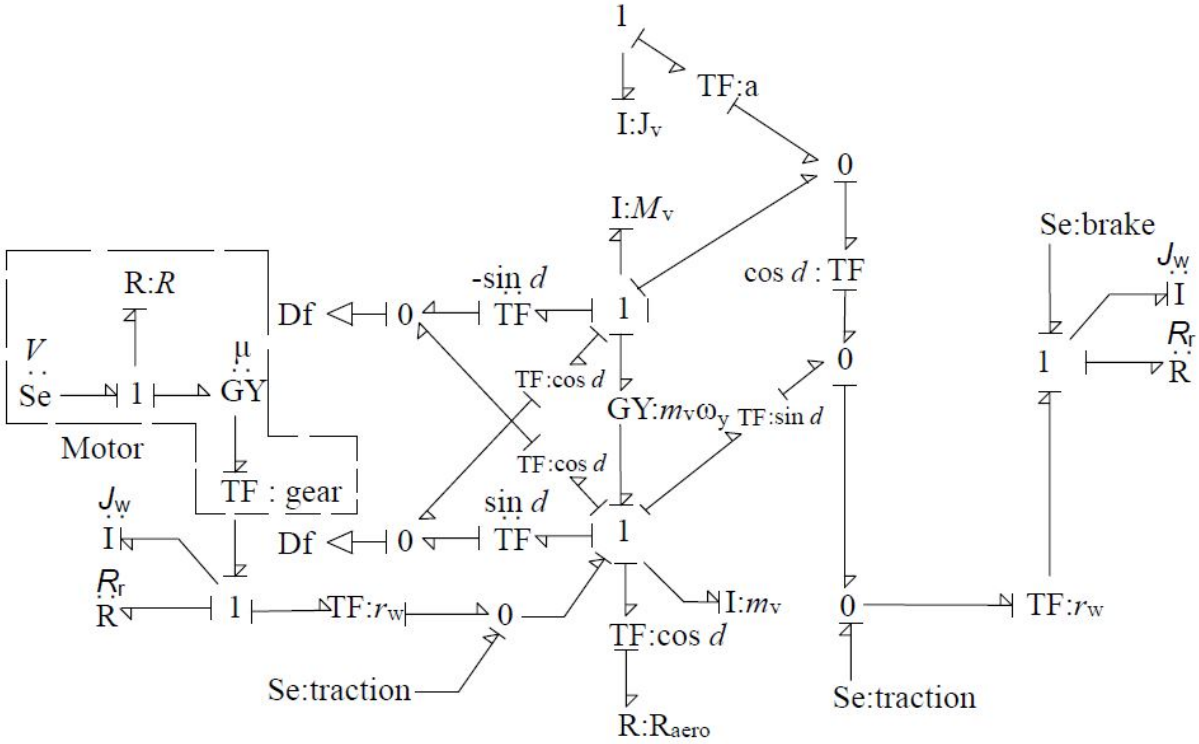

Fig. 3.17 Reduced bond graph of bicycle model without steering

3.5.4 Parameter values and simulation results

The parameters used for simulating the results are shown in Table 3.3.

Table 3.3 Parameter values of bicycle model with steering

Parameter values of bicycle model			
Vehicle body			
m_v	1600 kg	J_{cv}	1110 kg m^2
a	0.9 m	b	1.5 m
Wheel			
M_w	15 kg	J_{wy}	0.2 kg m^2
r_w	0.3 m	C_{rr}	0.01
Motor			
R	0.1 ohm	μ	2
V	175 V		
Steering			
δ	0.1 rad		

Results from the full and the reduced model were compared on the basis of the longitudinal vehicle velocity. For the initial straight line motion, the comparison is shown in

Fig. 3.18. Figure 3.18(a) and 3.18 (b) show the variation in longitudinal velocity in full and reduced system model, respectively. Figure 3.18(c) and 3.18(d) show the absolute and percentage error in the vehicle velocity calculated by the reduced model. The maximum percentage error is 0.0021%. This error is within the acceptable limit.

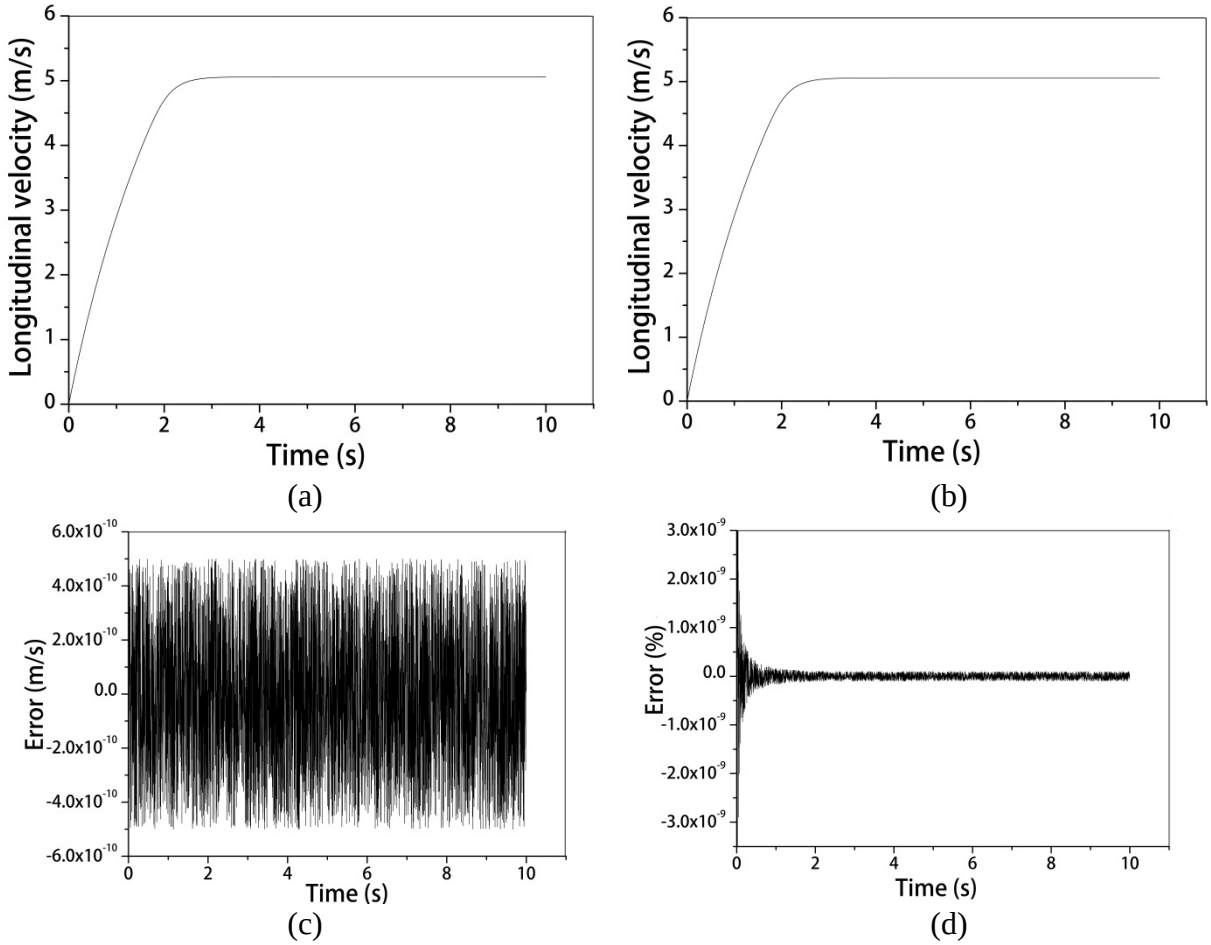

Fig. 3.18 Comparison of longitudinal velocity in full and reduced bicycle model without steering

Table 3.4 tabulates the role of various elements of model at various stages of trajectory for the discussed examples.

Table 3.4 Role of various elements during trajectory

Element	**Time**				
	0–10 s	10–10.4 s	10.4–10.7 s	10.7–10.9 s	10.9–12 s
R_1	Removed	Removed	Used	Used	Used
R_2	Removed	Removed	Removed	Used	Used
R_r	Used	Used	Used	Used	Removed

The full and reduced systems were simulated using parameters in Table 3.3. For steering motion models were again compared for variation in longitudinal velocity. Figure 3.19 shows comparison of full and reduced model during steering. The reduced model has a maximum error of 25%. This can be attributed to the fact that longitudinal velocity of vehicle was nearly zero. As the absolute error is within limits, this error can be neglected.

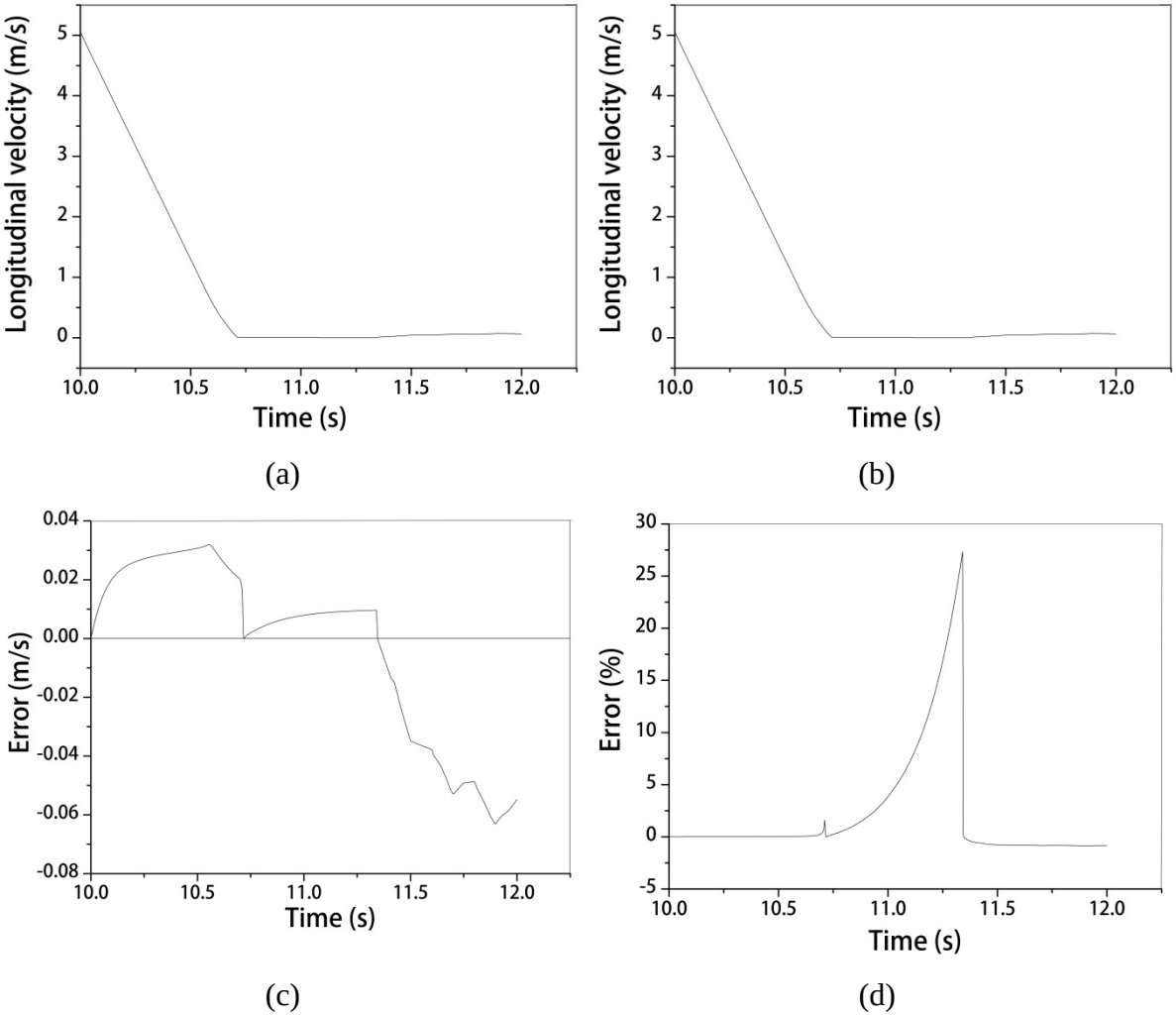

Fig. 3.19 Comparison of longitudinal velocity in full and reduced bicycle model during steering

CHAPTER 4 EIGENVALUE SENSITIVITY METHOD

4.1 METHOD

According to Eigenvalue sensitivity method, first the Eigenvalues of the system are found out and then the sensitivity of Eigenvalues for all the energy storing and energy dissipating elements are calculated. This provides the relative importance of every element for any given Eigenvalue. As I, C and R elements have different scales of magnitude they must be weighed in separate groups. Knowing the exact location of Eigenvalues gives a better control over the process; this is a major advantage over the Eigenvalue separation technique. Also, a major portion of this process can be automated.

4.2 PROCEDURE

Procedure as discussed in [**34**] is as follows

1) Find the matrix *S* and *L* such that

$$z = Sx \tag{4.1}$$

- *x* is generalized momentum/displacement vector
- *z* is corresponding flow/effect vector
- *S* is a diagonal matrix of the form $[s_1, s_2, \ldots, s_n]$ where $s_i = C_i \; or \; 1/I_i$ if ith energy storage element is capacitive or an inertial element.

$$d_{\text{out}} = L\, d_{\text{in}} \tag{4.2}$$

- d_{out} and d_{in} are the causal output and input of jth energy dissipation element.
- *L* is a diagonal matrix of the form $[l_1, l_2, \ldots, l_n]$ where $l_j = R_j \; or \; 1/R_j$ if jth energy dissipation element has flow or effort as causal input.

2) Find the connectivity matrices J_{SS} , J_{LL}, J_{SL} and J_{LS}
   - *S* represents energy storage elements.
   - *L* represents energy dissipating elements
   - J_{ij} is a connectivity matrix from the output of jth element to the input of ith element
3) Find matrix *A* such that

$$A = \left[J_{SS} + J_{SL}\, L \left(I - J_{LL}\right)^{-1} J_{LS}\right] S \tag{4.3}$$

4) Calculate the Eigenvalues of state matrix *A*.
5) Calculate *U* and *V* i.e. right and left eigenvector matrices for state matrix *A*.
6) For each Eigenvalue, find their sensitivity with all elements as

$$\frac{\partial y_i}{\partial s_j} = v_i^T \left(J\, t_j\, e_j\, e_j^T \right) u_i \tag{4.4}$$

$$\frac{\partial y_i}{\partial s_j} = v_i^T \left(J_{SL} \frac{\partial L}{\partial l_j} (I - J_{LL} L)^{-1} J_{SL} S + J_{SL} L (I - J_{LL} L)^{-2} J_{LL} J_{LS} S \right) u_i \tag{4.5}$$

If $J_{LL}=0$

$$\frac{\partial y_i}{\partial s_j} = v_i^T \left(J_{SL}\, z_j\, e_j\, e_j^T\, J_{LS} S \right) u_i \tag{4.6}$$

t_j and z_j are multiplication factors given in Table 4.1.

Table 4.1 Multiplication factors

Domain	R-element	$z = \frac{\partial R}{\partial l}$	I-element	$t_j = \frac{\partial I}{\partial s}$	C-element	$t_j = \frac{\partial C}{\partial s}$
Mechanical translation	b	1	$\frac{1}{m}$	$-\frac{1}{m^2}$	k	1
Mechanical rotation	c	1	$\frac{1}{J}$	$-\frac{1}{J^2}$	k	1
Hydraulic	R	1	$\frac{1}{I}$	$-\frac{1}{I^2}$	$\frac{1}{C}$	$-\frac{1}{C^2}$
Electrical	R	1	$\frac{1}{L}$	$-\frac{1}{L^2}$	$\frac{1}{C}$	$-\frac{1}{C^2}$

7) Find the absolute value of $\frac{\partial \lambda_i}{\partial s_j}$ and $\frac{\partial \lambda_i}{\partial l_j}$. Then arrange them in the form of matrices

$$E_{IC} = \begin{bmatrix} \left|\frac{\partial \lambda_1}{\partial s_1}\right| & \left|\frac{\partial \lambda_1}{\partial s_2}\right| & \cdots & \left|\frac{\partial \lambda_1}{\partial s_n}\right| \\ \left|\frac{\partial \lambda_2}{\partial s_1}\right| & \left|\frac{\partial \lambda_2}{\partial s_2}\right| & \cdots & \left|\frac{\partial \lambda_1}{\partial s_n}\right| \\ \vdots & \vdots & \cdots & \vdots \\ \left|\frac{\partial \lambda_n}{\partial s_1}\right| & \left|\frac{\partial \lambda_n}{\partial s_2}\right| & \cdots & \left|\frac{\partial \lambda_n}{\partial s_n}\right| \end{bmatrix} \quad and \quad E_R = \begin{bmatrix} \left|\frac{\partial \lambda_1}{\partial l_1}\right| & \left|\frac{\partial \lambda_1}{\partial l_2}\right| & \cdots & \left|\frac{\partial \lambda_1}{\partial l_m}\right| \\ \left|\frac{\partial \lambda_2}{\partial l_1}\right| & \left|\frac{\partial \lambda_2}{\partial l_2}\right| & \cdots & \left|\frac{\partial \lambda_1}{\partial l_m}\right| \\ \vdots & \vdots & \cdots & \vdots \\ \left|\frac{\partial \lambda_n}{\partial l_1}\right| & \left|\frac{\partial \lambda_n}{\partial l_2}\right| & \cdots & \left|\frac{\partial \lambda_n}{\partial l_m}\right| \end{bmatrix} \tag{4.7}$$

4.2.1 Finding the connectivity matrix

The connectivity matrix between different elements can be found out by drawing the signal flow graph of the system from the bond graph model, but as the complexity of system grows it becomes difficult to handle a very large signal flow graph. Connectivity matrix can be

directly obtained from the bond graph model by the following rules. The procedure is similar to tracing the signal flow graph.

Rules:

Only those elements are considered connected if they can be linked to each other by a causal path.

1) J_{SS} is a skew symmetric matrix; so, calculate only the upper triangular or the lower triangular elements.
2) $J_{SL} = -J_{LS}^{T}$ so, calculate one of these two matrices.
3) Depending on whether the element output to system is flow or effort, the behaviour of intermediate points on the causal path is checked.

Procedure:

1) Take the connectivity equal to 1. Multiply this with factors imposed by the junctions.
2) 1 Junction:
   a) For flow output factor is 1.
   b) For effort output if the direction of entry and exit of information have similar power orientation i.e. either both into the system or both out from the system then the factor is -1, else the factor is 1.
3) 0 Junction:
   a) For effort output factor is 1.
   b) For flow output if the direction of entry and exit of information have similar power orientation i.e. either both into the system or both out from the system then the factor is -1, else the factor is 1.
4) Transformer

   In case of transformer element, the factor is η if following same direction of power and 1/η if following opposite direction of power, where η is the transformer modulus.
5) Gyrator
   a) Factor is g, where g is the gyrator modulus.
   b) Sense of output changes from flow to effort and vice versa for the remaining path.
6) Activated bonds can be followed only if the activation is similar to the sense of path followed and the power direction is also in the same direction of path.

4.3 LIMITATIONS

The major limitation of this technique is that it is applicable only for linear time invariant (LTI) systems. A non-linear model can be reduced only after linearizing the model. The other major limitation is that the elements which are found to be least active from the calculations cannot be removed directly from the model as removing some elements may put the model in unstable state. So, such elements have to be restored manually at a later stage.

4.4 CASE STUDY I: BICYCLE SUSPENSION MODEL

4.4.1 Bond graph model of bicycle vehicle with suspension model

Bicycle model is an approximate model which is assumed to be symmetric about the longitudinal mid-plane. The model considers three degrees of freedom (DOF), with 2 translational DOF and 1 rotational DOF. The vehicle body, the front wheel and the rear wheel have three DOF while the front and rear suspensions have only 2 DOF i.e. 2 translational DOF.

The vehicle is considered as a rear wheel drive vehicle. A motor is used to run the wheel. The wheel also experiences tractive force. This tractive force is modelled using Pacejka's magic formula [**14**]. The power goes from the rear wheel to the vehicle body through the rear suspensions, from where it is distributed to the rest of the vehicle.

The mass of the body, wheels, stiffness and damping of the front and rear suspensions, moment of inertia of wheels about its lateral axis, moment of inertia of the vehicle body about a lateral axis passing through is centre of mass and stiffness and damping of the front and rear tires are used as parameters for modelling the system. All the parameters and motions are considered in the inertial frame.

The schematic diagram of the model is shown in Fig. 4.1. The line arrows show the allowed degrees of freedom for a part. The solid arrows show the traction force acting on the wheel. The blank arrows show the direction of power transmission within the system. In the bond graph model, the voltage applied to the motor is represented as Se-element (Source of effort). The resistive element in the motor converts it into flow and we get flow parameter for the system. The conversion of effort to flow is governed by Ohm's law. This electrical current is converted into rotational effort (torque) by the gyrator-element. The effort is scaled using a gearbox which is shown by a transformer-element.

The torque is fed to the rear wheel. Due to the moment of inertia of the wheel, we get equal flows around the 1 junction. This rotation flow is converted into linear flow using by a

transformer. The magnitude of the transformer coefficient is equal to the wheel radius. At this point, the effort moving the car is the traction, given by Eq. 3.15. So, a 0-junction which represents an equality of effort is used with an effort source.

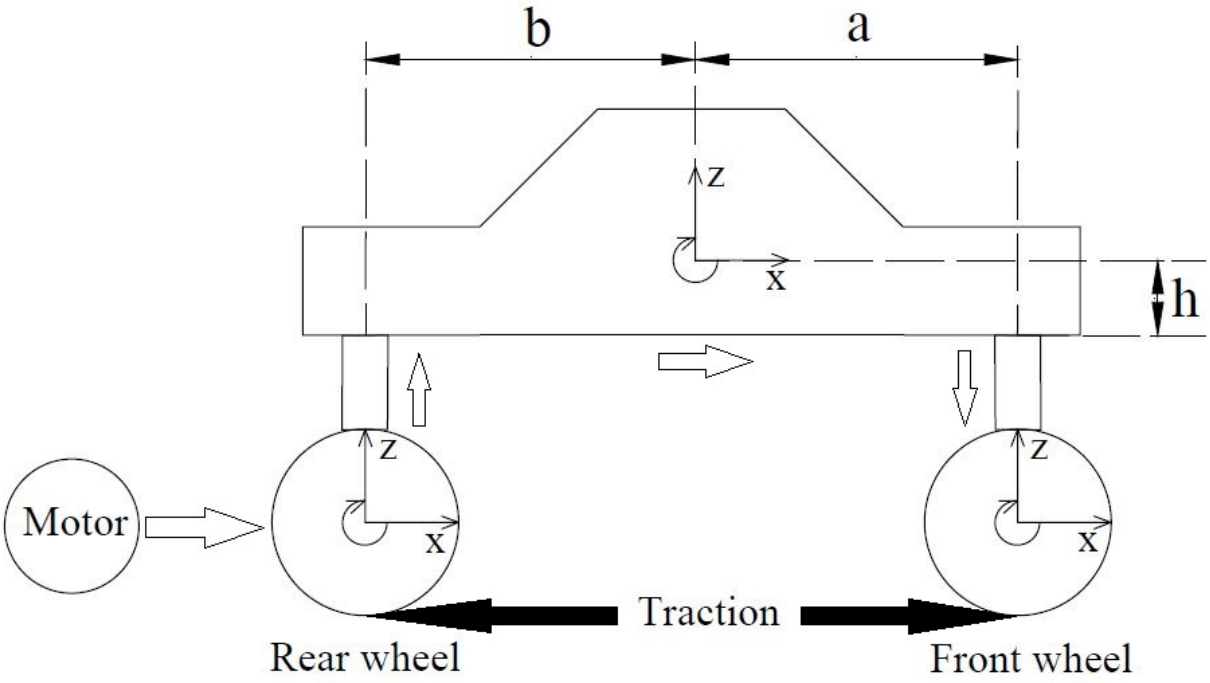

Fig. 4.1 Schematic diagram of bicycle model with suspension.

This effort (torque) acts on the wheel which propels it in the forward direction. The mass of the wheel gives the magnitude of linear flow. The flow is transferred from the wheel to the vehicle body, at a point just above the suspension. The suspension system provides stiffness and dissipation to the flow represented here by C and R-element, respectively.

The flow at this point is the summation of flows due to linear and rotation motions at the vehicle centre, so a 0-junction is used, which represents a summation of flows. The relation between velocities at centre and at point above wheel is given by

$$\dot{x}_p = \dot{x}_c + \alpha\,\dot{\theta}_c \tag{4.8}$$

$$\dot{z}_p = \dot{z}_c + \beta\,\dot{\theta}_c \tag{4.9}$$

Where α is the displacement of point along z-axis and β is the displacement along x-axis. For front wheels α is equal to –h and β is a, while for rear wheels α is equal to –h and β is $-b$.

The tyre stiffness and resistance is also modelled and is put along the wheel mass acting along the y-direction. Similar connection is made for the front wheel. Figure 4.2 shows the bond graph model of the system.

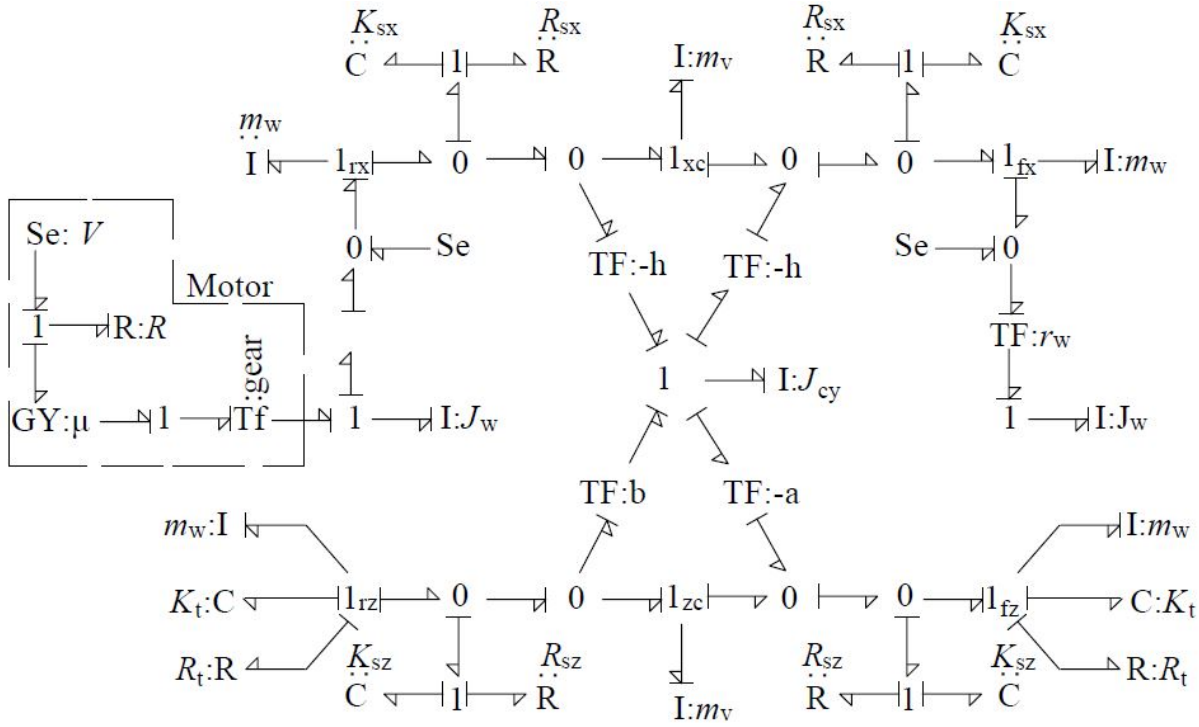

Fig. 4.2 Bond graph of bicycle model with suspension

4.4.2 Eigenvalue sensitivity technique in bicycle vehicle with suspension model

1) Using the procedure discussed, the various coefficient matrices and connectivity matrices were calculated

First the I-elements were modelled, so $S_i = 1/I$, for i between 1–9. Modelling of I-elements, was followed by modelling of C-elements so S_i=C for i between 10–15.

The coefficient matrices S and L were calculated as follows:

$$S = diag(0.06667, 0.06667, 0.000625, 0.000625, 0.0009009, 0.06667, 0.06667, 5, 5, 1e7, 80000, 1e7, 80000, 305000, 305000)$$

and

$$L = diag(2000, 500, 2000, 500, 200, 200, 0.1)$$

The connectivity matrices calculated using the procedure discussed in Sub-section 4.2.1, are given as:

$$J_{LS} = \begin{bmatrix} 1 & 0 & -1 & 0 & 10 & 0 & 0 & 0 & 0 & 0 & 0 & 0 & 0 & 0 & 0 \\ 0 & 1 & 0 & -1 & -0.667 & 0 & 0 & 0 & 0 & 0 & 0 & 0 & 0 & 0 & 0 \\ 0 & 0 & 1 & 0 & -0.1 & -1 & 0 & 0 & 0 & 0 & 0 & 0 & 0 & 0 & 0 \\ 0 & 0 & 0 & 1 & -0.9 & 0 & -1 & 0 & 0 & 0 & 0 & 0 & 0 & 0 & 0 \\ 0 & 0 & 0 & 0 & 0 & 0 & 1 & 0 & 0 & 0 & 0 & 0 & 0 & 0 & 0 \\ 0 & 1 & 0 & 0 & 0 & 0 & 0 & 0 & 0 & 0 & 0 & 0 & 0 & 0 & 0 \\ 0 & 0 & 0 & 0 & 0 & 0 & 0 & -1 & 0 & 0 & 0 & 0 & 0 & 0 & 0 \end{bmatrix}$$

$$J_{SS} = \begin{bmatrix} 0 & 0 & 0 & 0 & 0 & 0 & 0 & 0 & 0 & -1 & 0 & 0 & 0 & 0 & 0 \\ 0 & 0 & 0 & 0 & 0 & 0 & 0 & 0 & 0 & 0 & -1 & 0 & 0 & 0 & -1 \\ 0 & 0 & 0 & 0 & 0 & 0 & 0 & 0 & 0 & 1 & 0 & -1 & 0 & 0 & 0 \\ 0 & 0 & 0 & 0 & 0 & 0 & 0 & 0 & 0 & 0 & 1 & 0 & -1 & 0 & 0 \\ 0 & 0 & 0 & 0 & 0 & 0 & 0 & 0 & 0 & -10 & 0.667 & 0.1 & 0.9 & 0 & 0 \\ 0 & 0 & 0 & 0 & 0 & 0 & 0 & 0 & 0 & 0 & 0 & 1 & 0 & 0 & 0 \\ 0 & 0 & 0 & 0 & 0 & 0 & 0 & 0 & 0 & 0 & 0 & 0 & 1 & -1 & 0 \\ 0 & 0 & 0 & 0 & 0 & 0 & 0 & 0 & 0 & 0 & 0 & 0 & 0 & 0 & 0 \\ 0 & 0 & 0 & 0 & 0 & 0 & 0 & 0 & 0 & 0 & 0 & 0 & 0 & 0 & 0 \\ 1 & 0 & -1 & 0 & 10 & 0 & 0 & 0 & 0 & 0 & 0 & 0 & 0 & 0 & 0 \\ 0 & 1 & 0 & -1 & -0.667 & 0 & 0 & 0 & 0 & 0 & 0 & 0 & 0 & 0 & 0 \\ 0 & 0 & 0 & 1 & -0.1 & 0 & 0 & 0 & 0 & 0 & 0 & 0 & 0 & 0 & 0 \\ 0 & 0 & 0 & 1 & -0.9 & 0 & -1 & 0 & 0 & 0 & 0 & 0 & 0 & 0 & 0 \\ 0 & 0 & 0 & 0 & 0 & 0 & 1 & 0 & 0 & 0 & 0 & 0 & 0 & 0 & 0 \\ 0 & 1 & 0 & 0 & 0 & 0 & 0 & 0 & 0 & 0 & 0 & 0 & 0 & 0 & 0 \end{bmatrix}$$

$$J_{SL} = \begin{bmatrix} -1 & 0 & 0 & 0 & 0 & 0 \\ 0 & -1 & 0 & 0 & -1 & 0 \\ 1 & 0 & -1 & 0 & 0 & 0 \\ 0 & 1 & 0 & -1 & 0 & 0 \\ -10 & 0.667 & 0.1 & 0.9 & 0 & 0 \\ 0 & 0 & 0 & 0 & 0 & 0 \\ 0 & 0 & 0 & 1 & 0 & 0 \\ 0 & 0 & 0 & 0 & 0 & 1 \\ 0 & 0 & 0 & 0 & 0 & 0 \\ 0 & 0 & 0 & 0 & 0 & 0 \\ 0 & 0 & 0 & 0 & 0 & 0 \\ 0 & 0 & 0 & 0 & 0 & 0 \\ 0 & 0 & 0 & 0 & 0 & 0 \\ 0 & 0 & 0 & 0 & 0 & 0 \end{bmatrix}$$

J_{LL} for this system is an empty set.

2) Using the above matrices the Eigenvalues of the system were calculated. The calculated Eigenvalues are listed and plotted as :

$\lambda_{1,2} = -157.57 \pm 1244.704$

$\lambda_{3,4} = -67.27 \pm 817.4487i$

$\lambda_{5,6} = -23.37 \pm 158.506i$

$\lambda_{7,8} = -23.44 \pm 158.516i$

$\lambda_{9,10} = -0.20381 \pm 8.955i$

$\lambda_{11,12} = -0.075 \pm 5.4362\text{i}$

$\lambda_{13} = 1.36e-14$

$\lambda_{14} = -0.5$

$\lambda_{15} = 0$

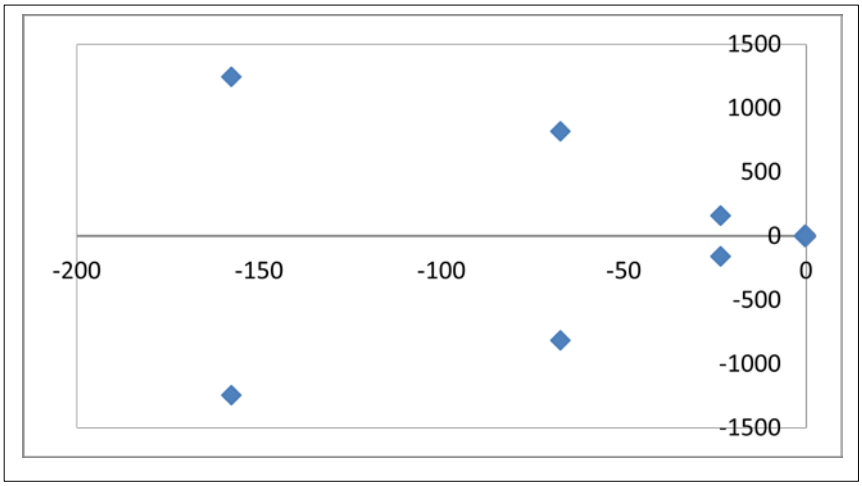

Fig 4.3 Eigenvalue distribution in bicycle model with suspension

As, the actual location of Eigenvalues is known, it is assumed that as $\lambda_{1,2,3,4}$ have very high real component in compared to the others, their effect will dissipate very soon; so, the system is reduced by neglecting these Eigenvalues. Also, $\lambda_{13,\,15}$ are nearly equal to zero, they do not add to the dynamic component and can be neglected. For achieving this, the effects matrices of components are analyzed.

The elements of the effect matrices, as discussed previously are the measure of sensitivity of Eigenvalue to an element. By performing some suitable operations on the matrices, the relative importance of the elements for some specific Eigenvalue can be obtained. For this case, the three different types of elements were compared separately. This gives three different effect matrices, instead of two as I and C elements were clubbed together in given procedure. For comparison to be only among one type of elements, the elements in every row of sensitivity matrices are divided by the biggest element in that row. This gives relative importance of each element for any particular Eigenvalue. As it is already assumed that some Eigenvalues can be neglected, the rows of the effect matrices, corresponding to these Eigenvalues are dropped completely. Also, elements are rounded off to four decimal places.

3) The effect matrices were found using the matrices calculated in the step 1.

After operations and neglecting the selected Eigenvalues, the effect matrix obtained is as follows:

$$Ef_I = \begin{bmatrix} 0.0005 & 1 & 0.0005 & 0.0018 & 0.0263 & 0 & 0.7091 & 0 & 0 \\ 0.0005 & 1 & 0.0005 & 0.0018 & 0.0263 & 0 & 0.7091 & 0 & 0 \\ 0 & 0.7091 & 0 & 0.2525 & 0.0014 & 0 & 1 & 0 & 0 \\ 0 & 0.7091 & 0 & 0.2525 & 0.0014 & 0 & 1 & 0 & 0 \\ 0.0001 & 0 & 0.0001 & 1 & 0.0063 & 0 & 0 & 0 & 0 \\ 0.0001 & 0 & 0.0001 & 1 & 0.0063 & 0 & 0 & 0 & 0 \\ 0.0179 & 0 & 0.0179 & 0.0719 & 1 & 0 & 0 & 0 & 0 \\ 0.0179 & 0 & 0.0179 & 0.0719 & 1 & 0 & 0 & 0 & 0 \\ 0 & 0 & 0 & 0 & 0 & 0 & 0 & 1 & 0 \end{bmatrix}$$

$$Ef_C = \begin{bmatrix} 0 & 1 & 0 & 0.7091 & 0.7068 & 0.9968 \\ 0 & 1 & 0 & 0.7091 & 0.7068 & 0.9968 \\ 0 & 0.7091 & 0 & 1 & 0.9913 & 0.7029 \\ 0 & 0.7091 & 0 & 1 & 0.9913 & 0.7029 \\ 0 & 0.7007 & 0 & 1 & 0.6940 & 0.0486 \\ 0 & 0.7007 & 0 & 1 & 0.6940 & 0.0486 \\ 0 & 1 & 0 & 0.7007 & 0.0483 & 0.0690 \\ 0 & 1 & 0 & 0.7007 & 0.0483 & 0.0690 \\ 0 & 0 & 0 & 0 & 0 & 0 \end{bmatrix}$$

$$Ef_R = \begin{bmatrix} 0 & 1 & 0 & 0.7091 & 0.7068 & 0.9968 & 0 \\ 0 & 1 & 0 & 0.7091 & 0.7068 & 0.9968 & 0 \\ 0 & 0.7091 & 0 & 1 & 0.9913 & 0.7029 & 0 \\ 0 & 0.7091 & 0 & 1 & 0.9913 & 0.7029 & 0 \\ 0 & 0.7007 & 0 & 1 & 0.0694 & 0.0486 & 0 \\ 0 & 0.7007 & 0 & 1 & 0.0694 & 0.0486 & 0 \\ 0 & 1 & 0 & 0.7007 & 0.0483 & 0.0690 & 0 \\ 0 & 1 & 0 & 0.7007 & 0.0483 & 0.0690 & 0 \\ 0 & 0 & 0 & 0 & 0 & 0 & 1 \end{bmatrix}$$

Ef_{I}, Ef_{C} and Ef_{R} show the relative importance of I, C and R elements respectively for the selected Eigenvalues. By comparison it is found that some columns have low magnitude. The elements corresponding to those columns are neglected and a reduced system is obtained. This reduced system is modelled using the bond graph technique and the results are compared between the full and reduced system.

4.4.3 Reduced Model

From matrix Ef_{I}, it is observed that first and third columns have all the elements of very low magnitude. This means that these elements contribute very less compared to others selected Eigenvalues; hence, they can be neglected and removed from the model.

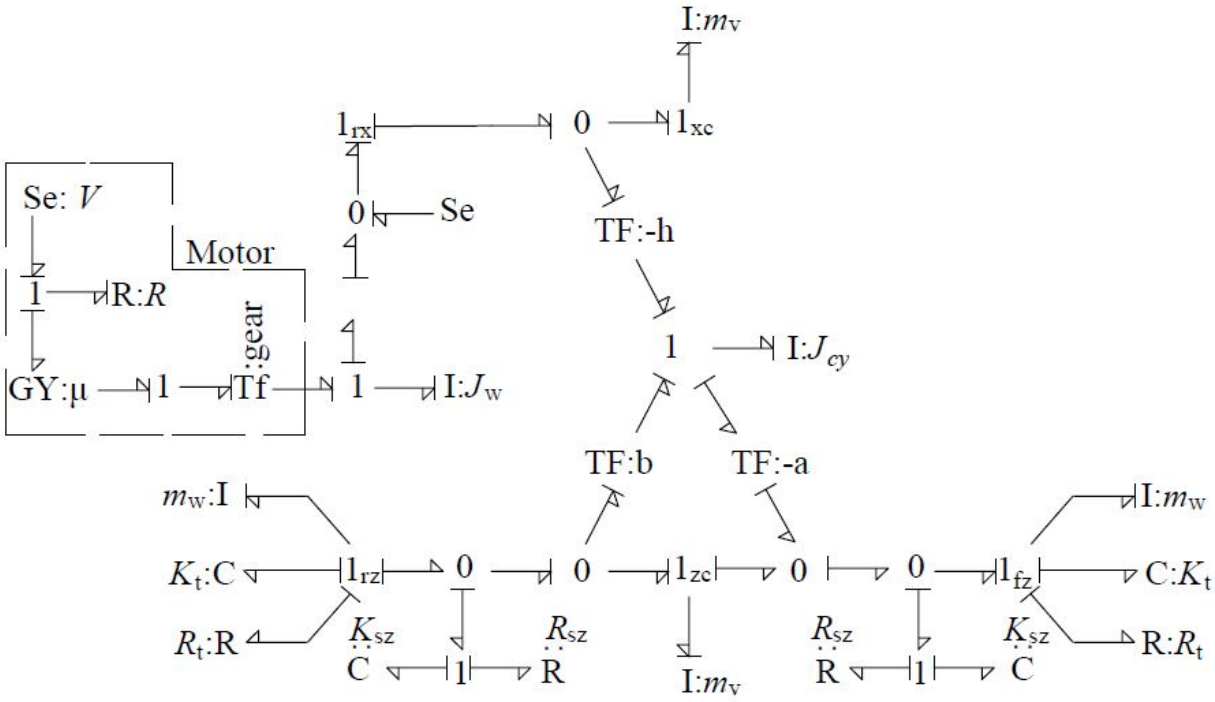

Fig. 4.4 Reduced bond graph of bicycle model with suspension

Similarly, the first and third columns of Ef_C and Ef_R also have very low magnitude; hence, these elements can also be neglected. The reduced model of the system is obtained by removing these elements from the system. The bond graph of the reduced model is shown in Fig. 4.4.

4.4.4 Parameter values and simulation results

The vehicle parameters are given in Table 4.2.

Table 4.2 Parameters used for simulation of bicycle model with suspension

Parameter Values for bicycle suspension model					
Vehicle body					
m_v	1600 kg	J_{cy}	1110 kg m_2	a	0.9 m
b	1.5 m				
Wheel					
m_w	15 kg	J_{wy}	0.2 kg m^2	r_w	0.3 m
Tyre					
R_t	200 N/m	K_t	305 kN/m		
Suspension					
K_{sx}	10^7 N/m	R_{sx}	2000 N/m		
K_{sz}	80000 N/m	R_{sz}	500 N/m		

Figure 4.5 shows the comparison of full and reduced model by comparing the pitch angle observed at the center of mass of the vehicle body. It is observed that reduced model gives results very close to the full model. The percentage error becomes high if pitch angle becomes close to 0, but this high percentage error can be neglected as the absolute error is negligible.

Figure 4.6 compares the full and reduced model by considering the vehicle velocity. Fig. 4.6(d) shows the variation in percentage error of the reduced system. The maximum percentage error of nearly 2% is observed. Hence, the reduced model conserves the longitudinal dynamics of the system.

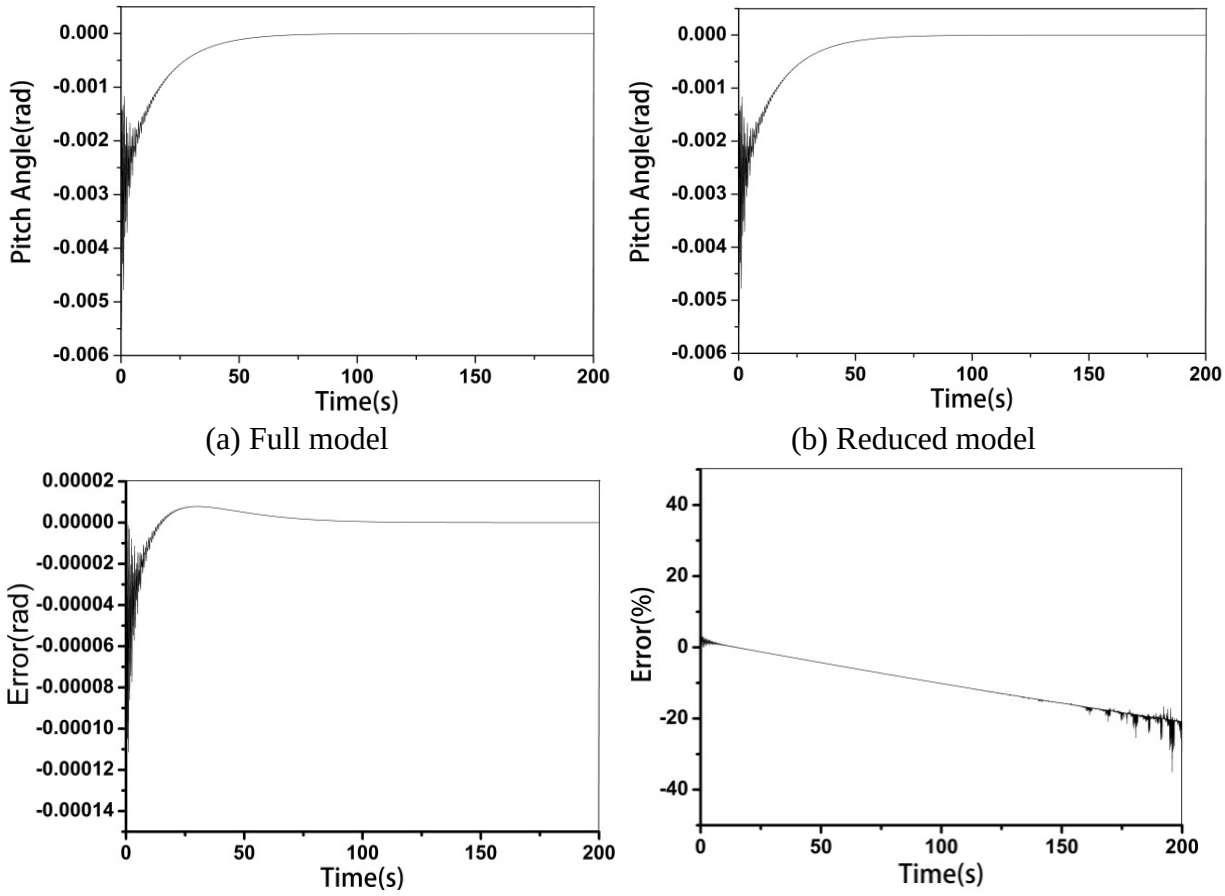

(a) Full model (b) Reduced model

(c) Absolute error (d) Percentage error

Fig 4.5 Comparison of pitch angle in the full and reduced bicycle model with suspension

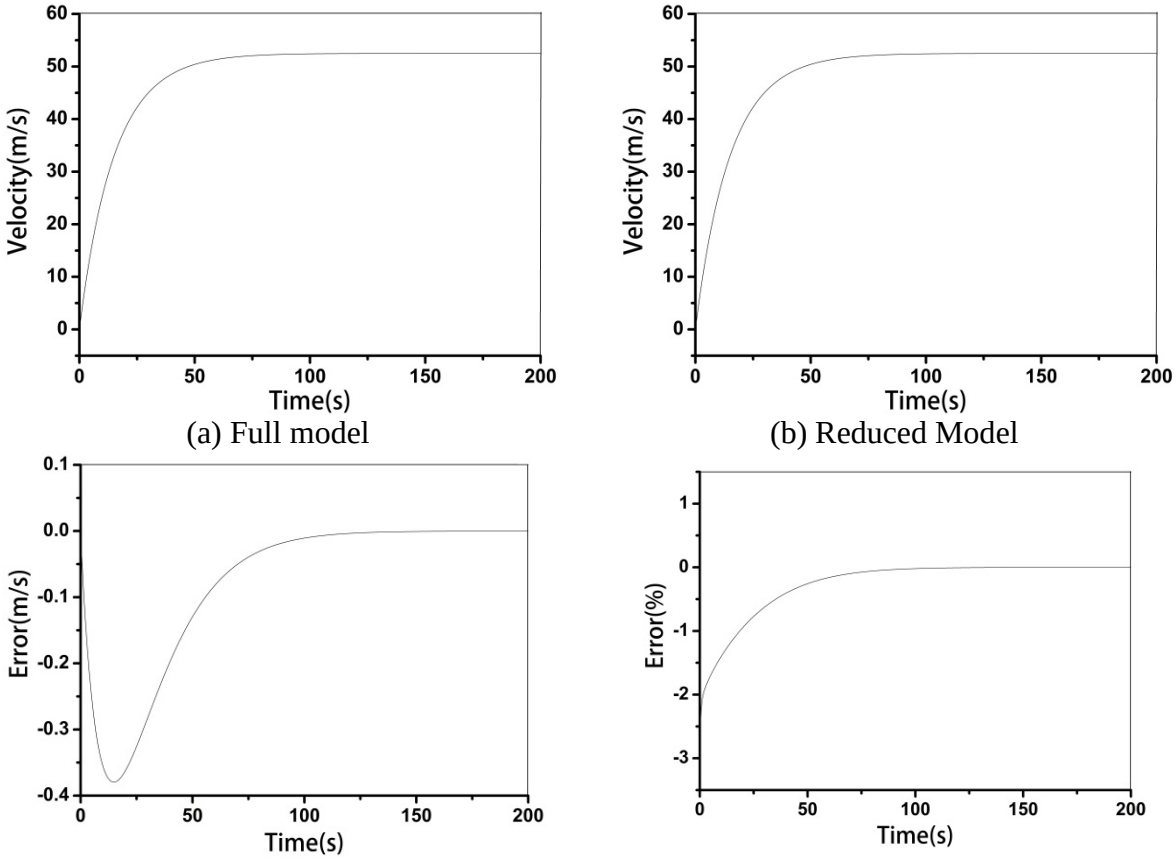

(a) Full model (b) Reduced Model

(c) Absolute error (d) Percentage error

Fig 4.6 Comparison of longitudinal velocity in full and reduced bicycle model with suspensions

4.5 CASE STUDY II: FOUR WHEEL MODEL

4.5.1 Bond graph model of four wheel vehicle model

The four wheel dynamic model consists of six basic components i.e. the vehicle body, suspensions, wheels, differential, steering and ABS. The word bond graph of a four wheel vehicle model is shown in Fig. 4.7. The vehicle body and the wheels are considered to be in non-inertial frame, while the suspensions are considered in the inertial frame. So, the components are connected to each other through various coordinate transformations.

The vehicle body and wheels are modelled with all six degrees of freedom. A coordinate frame is attached to the center of mass of the wheels and vehicle body which moves with the body it is attached to. Hence, the coordinate frame is a non-inertial frame. The dynamics of these bodies is defined using the Newton-Euler equations, which are as follows:

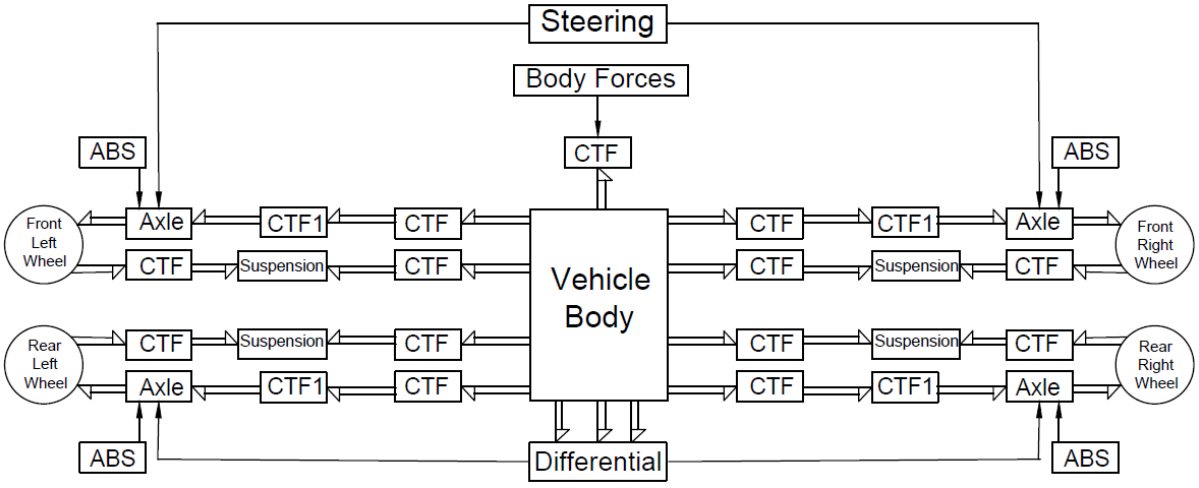

Fig. 4.7 Word bond graph model of four wheel vehicle model [**35**]

$$\sum F_{\mathrm{X}} = m_{\mathrm{c}}\ddot{x}_{\mathrm{c}} + m_{\mathrm{c}}(\dot{z}_{\mathrm{c}}\dot{\theta}_{\mathrm{cy}} - \dot{y}_{\mathrm{c}}\dot{\theta}_{\mathrm{cz}}) \tag{4.11}$$

$$\sum F_{\mathrm{Y}} = m_{\mathrm{c}}\ddot{y}_{\mathrm{c}} + m_{\mathrm{c}}(\dot{x}_{\mathrm{c}}\dot{\theta}_{\mathrm{cz}} - \dot{z}_{\mathrm{c}}\dot{\theta}_{\mathrm{cx}}) \tag{4.12}$$

$$\sum F_{\mathrm{Z}} = m_{\mathrm{c}}\ddot{z}_{\mathrm{c}} + m_{\mathrm{c}}(\dot{y}_{\mathrm{c}}\dot{\theta}_{\mathrm{cx}} - \dot{x}_{\mathrm{c}}\dot{\theta}_{\mathrm{cy}}) \tag{4.13}$$

$$\sum M_{\mathrm{X}} = J_{\mathrm{cx}}\ddot{\theta}_{\mathrm{cx}} - \dot{\theta}_{\mathrm{cy}}\dot{\theta}_{\mathrm{cz}}(J_{\mathrm{cy}} - J_{\mathrm{cz}}) \tag{4.14}$$

$$\sum M_{\mathrm{Y}} = J_{\mathrm{cy}}\ddot{\theta}_{\mathrm{cy}} - \dot{\theta}_{\mathrm{cz}}\dot{\theta}_{\mathrm{cx}}(J_{\mathrm{cz}} - J_{\mathrm{cx}}) \tag{4.15}$$

$$\sum M_{\mathrm{Z}} = J_{\mathrm{cz}}\ddot{\theta}_{\mathrm{cz}} - \dot{\theta}_{\mathrm{cx}}\dot{\theta}_{\mathrm{cy}}(J_{\mathrm{cx}} - J_{\mathrm{cy}}) \tag{4.16}$$

The equations 4.11–4.16 are implemented in the bond graph model using Newton-Euler junction structure shown in Fig. 4.8. The Newton-Euler junction structure consists of two triangles. One triangle represents the Newton's equations which provide linear dynamics and the other triangle represents the Euler equations which result in the rotary dynamics. Each triangle has a 1-junction at the corner. I-element is connected to the 1-junction. I-elements, represent the linear and rotary inertia in the three directions, in their respective rings. Different I-elements are coupled to each other through gyrator elements. Initially the body fixed frames are aligned with the rigid frames.

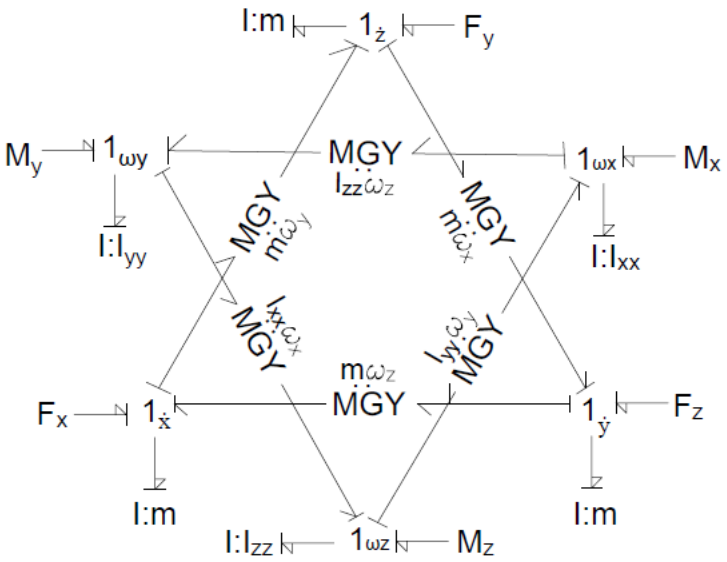

Fig. 4.8 Newton-Euler junction structure [**35**]

The Euler angles required for various transformations are calculated by integrating the Euler angle rates which are calculated as

$$\begin{Bmatrix} \dot{\phi} \\ \dot{\theta} \\ \dot{\psi} \end{Bmatrix} = \begin{bmatrix} 1 & 0 & -\sin\theta \\ 0 & \cos\phi & \cos\theta\sin\phi \\ 0 & -\sin\phi & \cos\theta\cos\phi \end{bmatrix}^{-1} \begin{Bmatrix} \omega_x \\ \omega_y \\ \omega_z \end{Bmatrix} \tag{4.17}$$

$$\begin{Bmatrix} \dot{\phi} \\ \dot{\theta} \\ \dot{\psi} \end{Bmatrix} = \begin{bmatrix} 1 & \tan\theta\sin\phi & \tan\theta\cos\phi \\ 0 & \cos\phi & -\sin\phi \\ 0 & \sin\phi/\cos\theta & \cos\phi/\cos\theta \end{bmatrix} \begin{Bmatrix} \omega_x \\ \omega_y \\ \omega_z \end{Bmatrix} \tag{4.18}$$

After assigning various reference frames, the velocities at points just above the suspensions are found, before transforming them into inertial frames. The velocity components of the front left suspension point are given by Eq. 4.19 – 4.21. For geometric calculation, different nomenclatures were used with $x_1 = a$, $y_1 = c$ and $z_1 = -h$. Velocities for all the points above the suspensions are found in the similar manner.

$$\dot{x}_1 = \dot{x}_c + z_1\dot{\theta}_{cy} - y_1\dot{\theta}_{cz} \tag{4.19}$$

$$\dot{y}_1 = \dot{y}_c + x_1\dot{\theta}_{cz} - z_1\dot{\theta}_{cx} \tag{4.20}$$

$$\dot{z}_1 = \dot{z}_c + y_1\dot{\theta}_{cx} - x_1\dot{\theta}_{cy} \tag{4.21}$$

These velocities are then transformed from the non-inertial frame to the inertial frame using a transformation matrix. The equations for the transformations are given by Eq. 4.22. Eq. 4.22 represents the transformation block represented by CTF in word bond graph.

$$\begin{Bmatrix} \dot{X} \\ \dot{Y} \\ \dot{Z} \end{Bmatrix} = T \begin{Bmatrix} \dot{x} \\ \dot{y} \\ \dot{z} \end{Bmatrix} \tag{4.22}$$

$$T = \begin{bmatrix} \cos\psi & -\sin\psi & 0 \\ \sin\psi & \cos\psi & 0 \\ 0 & 0 & 1 \end{bmatrix} \begin{bmatrix} \cos\theta & 0 & \sin\theta \\ 0 & 1 & 0 \\ -\sin\theta & 0 & \cos\theta \end{bmatrix} \begin{bmatrix} 1 & 0 & 0 \\ 0 & \cos\phi & -\sin\phi \\ 0 & \sin\phi & \cos\phi \end{bmatrix} \tag{4.23}$$

The vehicle body experiences three sets of forces. The first are the body forces consisting of the weight and aerodynamic drag. The body forces act in the inertial frame, which are applied on the non-inertial frame of the body through a coordinate transformation. Second set of effort is the engine torque. Torque is applied on the wheels and is given to the vehicle body through two coordinate transformations; first from the non-inertial frame of the wheels to inertial frame of the suspensions and then to the non-inertial frame of the vehicle body. Finally, the forces and moments due to suspensions are the third kind. These forces act in the inertial frame and act on vehicle body through a transformation.

The bond graph model of showing connection of vehicle body to the front left wheel is shown in Fig. 4.9. The detailed modelling of wheel and CTF is not shown in Fig. 4.9. The bond graph undertakes only the equations used for finding the dynamics of the front left wheel. The remaining model can be modelled applying the similar kinematics on the vehicle body. The bond graph model shows the connection between the vehicle body and wheels through various coordinate transformations which are represented using Eq. 4.17–4.23 as discussed previously.

The wheels have six degrees of freedom and are placed in a non-inertial frame. The normal reaction due to tyre and road interaction as well as the weight of wheel act in the Z-direction of the inertial frame decoupling the vertical dynamics from the cornering and lateral dynamics. Longitudinal and cornering dynamic in the axle non-inertial frame are modulated by the ground reaction and wheel radius. The tyre stiffness and damping is provided to the vertical motion computed by adding various flows through transformers. The tyre and road interactions are represented by modulated resistance MR-element. Ports 1–6 shown in Fig. 4.10 are the bonds connected to the corresponding velocities in the suspension system. Port 7 is the source of external torque acting on the wheel either from differential or from braking system.

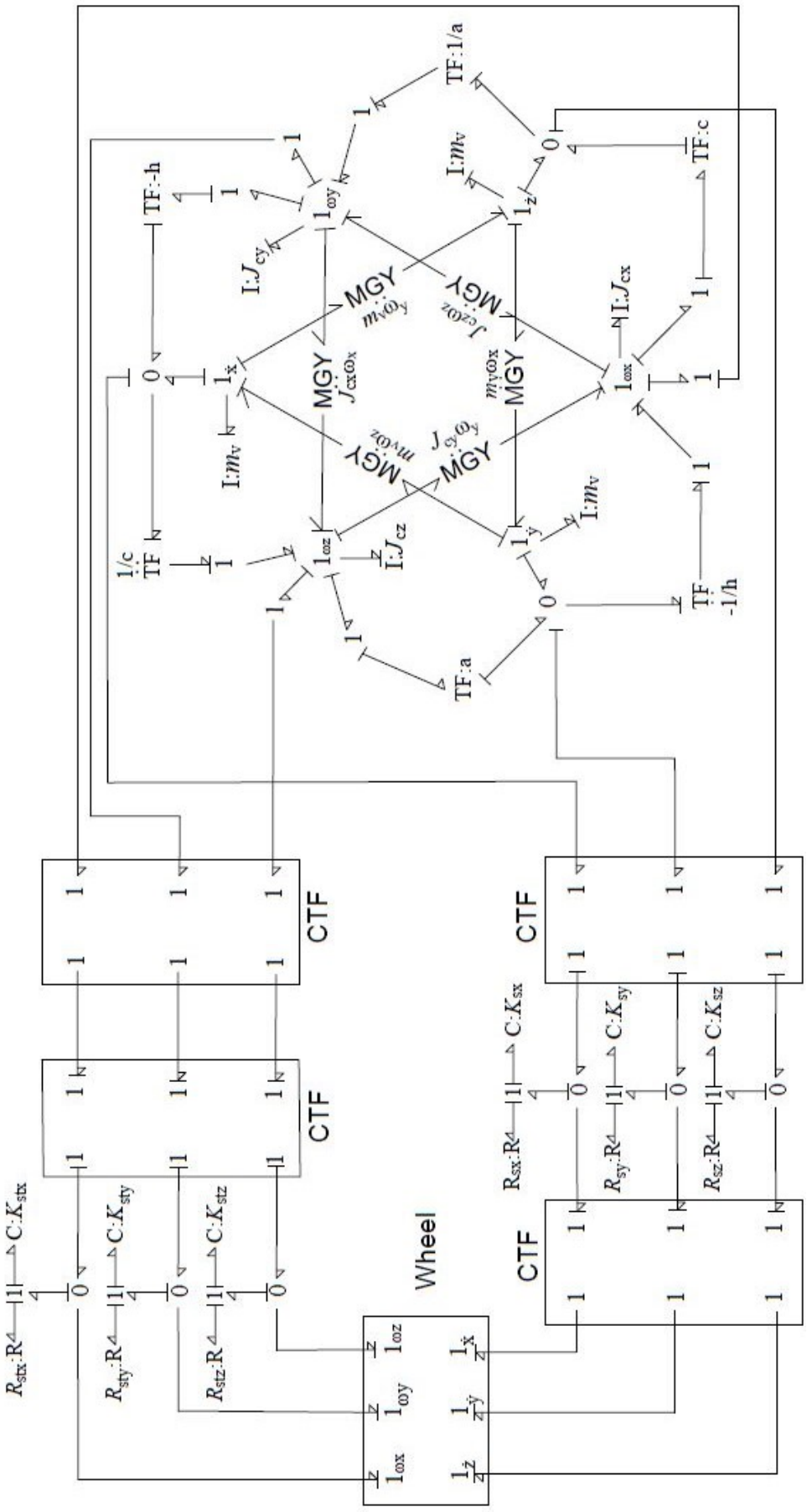

Fig. 4.9 Full bond graph of connection between vehicle body and front left wheel

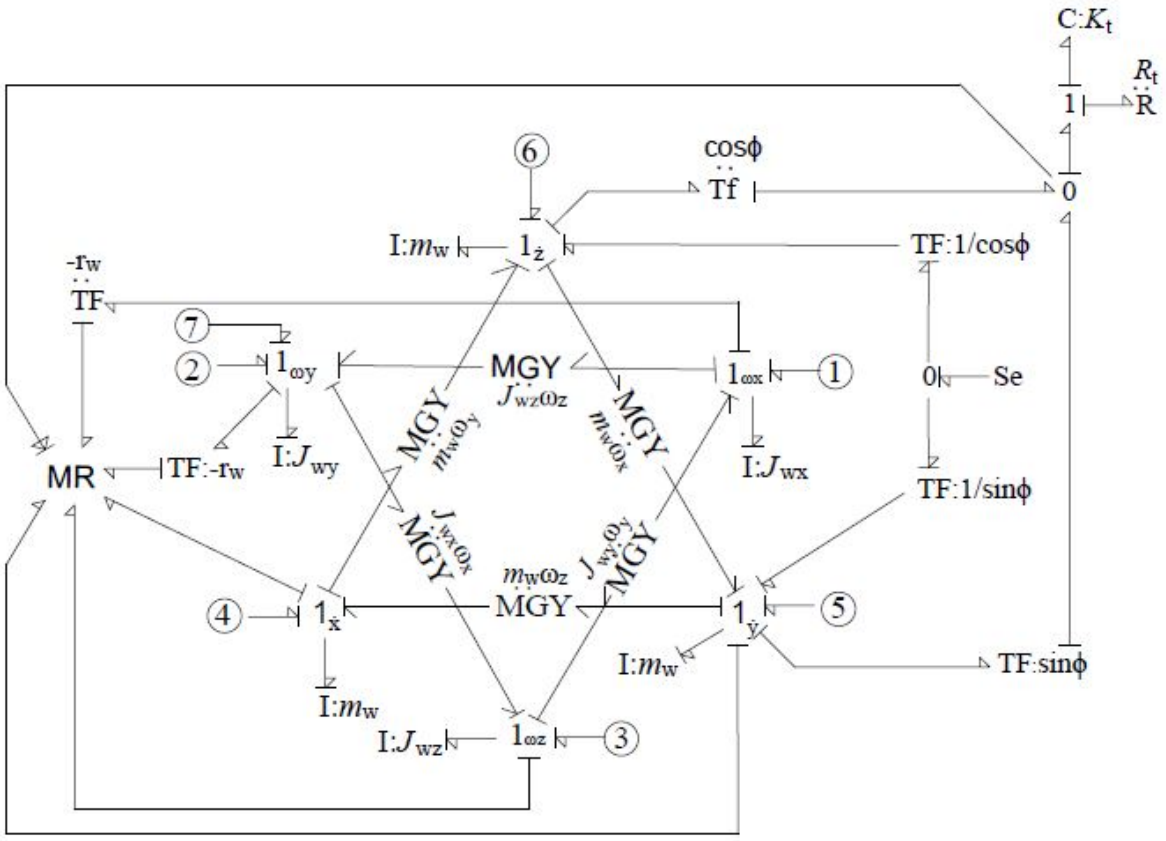

Fig. 4.10 Bond graph model of wheel used in full four wheel vehicle model [**35**]

The steering system is shown in Fig. 4.11. Torque (represented as effort source) is applied by the operator on the steering wheel. An inertial element J_{stw} represents the moment of inertia of the steering wheel. The transformer modulus μ is a mechanical transformation representing the ratio between the rotation of the steering wheel and actual steering rotation. The modulated transformer moduli m_i and m_o are calculated from the Ackerman steering geometry and are given by Eq. 4.24 and 4.25.

$$\dot{\delta}_i = \left[\frac{(a+b)\cos^2\theta_l + c\tan\theta_l \cos^2\theta_l}{(a+b)\cos^2\theta_{st} - c\tan\theta_{st}\cos^2\theta_{st}} \right] \dot{\delta} \tag{4.24}$$

$$\dot{\delta}_o = \left[\frac{(a+b)\cos^2\theta_r - c\tan\theta_r \cos^2\theta_r}{(a+b)\cos^2\theta_{st} + c\tan\theta_{st}\cos^2\theta_{st}} \right] \dot{\delta} \tag{4.25}$$

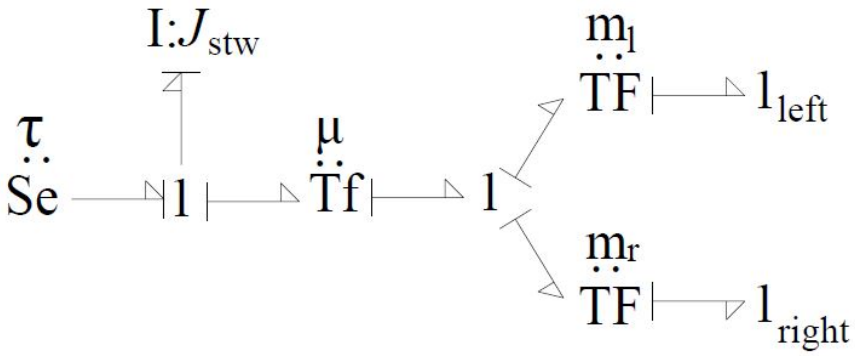

Fig 4.11 Bond graph of steering system used in four wheel model [**35**]

4.5.2 Handling non-linearity

It has been discussed previously that Eigenvalue sensitivity technique is applicable for LTI systems. But due to the presence of many modulated transformers and modulated gyrators in the system, this model is highly non-linear. Hence, to obtain a reduced model, the system must be linearized. There are two possible ways to linearize this system. The first option we have is to approximate, a very small change in the Euler angles, so that the trigonometric entities in the model are linearized. For practical purposes, such a system can hardly be of any use as the condition of very small change in angles can only be achieved if the time frame of calculation is very small. The other option is to obtain a reduced model, under conditions which lead to a nearly linear model. A condition of straight line motion was chosen to obtain a nearly linear mathematical model.

Under the condition of no steering many of the modulated transformers and gyrators attained a constant value. The rotation rate about y-axis in the various non-inertial coordinate systems did not die out; hence this component of model was not linearized. The variation of the body pitch angle in the body fixed frame with time is shown in Fig. 4.12.

To effectively reduce the model, the procedure was applied for the maximum, minimum and stable value. The maximum value was taken as 0.036 rad, the minimum value as -0.015 rad and the angle was assumed to stabilize at 0.00 rad. It was observed that all the three cases led to the same reduced model.

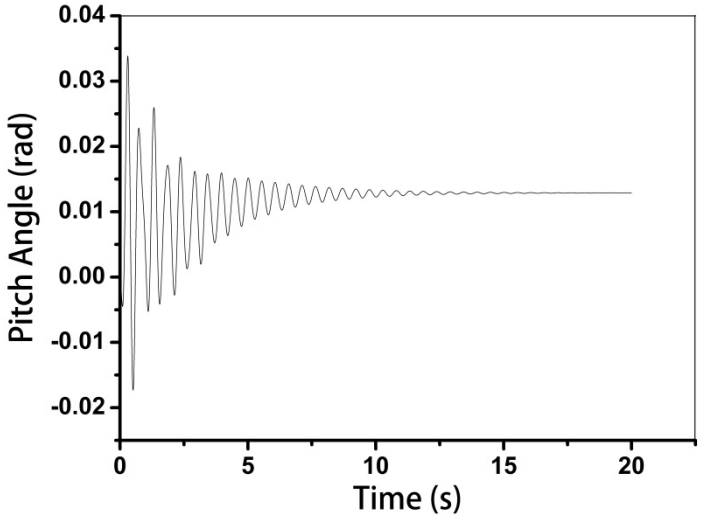

Fig. 4.12 Variation of vehicle pitch angle with time

4.5.3 Reduced model

The Eigenvalue sensitivity method was applied for the three cases in four wheel model. For all the cases the Eigenvalues with magnitudes greater than 10000 and those less than 1 were neglected. The conditioning procedure similar to the previous case was applied. The results for all the cases pointed to the same elements to be removed i.e. K_{sy} and R_{sy} from all the suspensions, K_{sty} and R_{sty} from the front axles, wheel mass acting along the y-direction and J_{wy} from the front wheels. But it is to be noted that the rotational components were pointed out by the algorithm only because of zero numerical value of the components, K_{sty} and R_{sty}. Hence, rotational components I_{sty}, K_{sty} and R_{sty} were not removed from the system. Another reason which led to the decision to include these components in the reduced model was that, removal of these components caused the system to be causally incorrect. So, removing these components would have also rendered the system unstable. Though the inertial element was removed, the mass of wheel acting along y-direction was not neglected to have more numerical accuracy. The connection was interpreted as a rigid link and the mass of the wheel was added numerically, to the mass of the vehicle body. Hence the inertial element representing the mass of vehicle body, now represented the mass of vehicle body and the wheels.

$$I = m_v + 4m_W \tag{4.26}$$

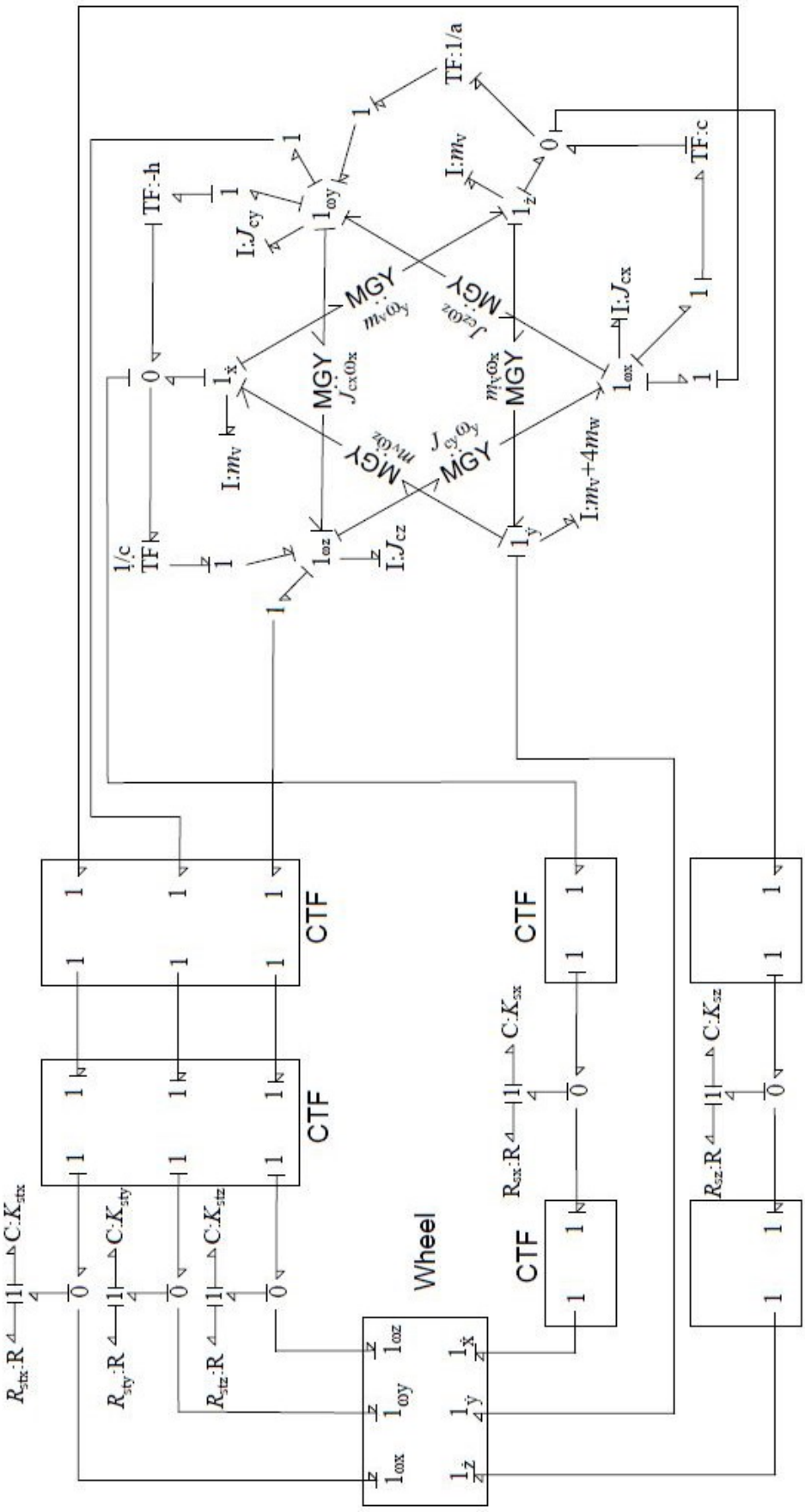

Fig. 4.13 Reduced bond graph of connection between vehicle body and front left wheel

Figure 4.13 shows the reduced bond graph of the vehicle body and the connection between the vehicle body and front left wheel. The suspension elements K_{sy} and R_{sy} were removed. The inertial elements of the wheel acting in the y-direction were connected directly to the inertial element of the vehicle body. Therefore, the effort input for wheel along y-axis was replaced with a flow source which indicates an equality of flow. This shows a physical connection between the wheel and vehicle body along the y-axis. Figure 4.14 shows the wheel model in reduced system. Port 5 now is a flow source.

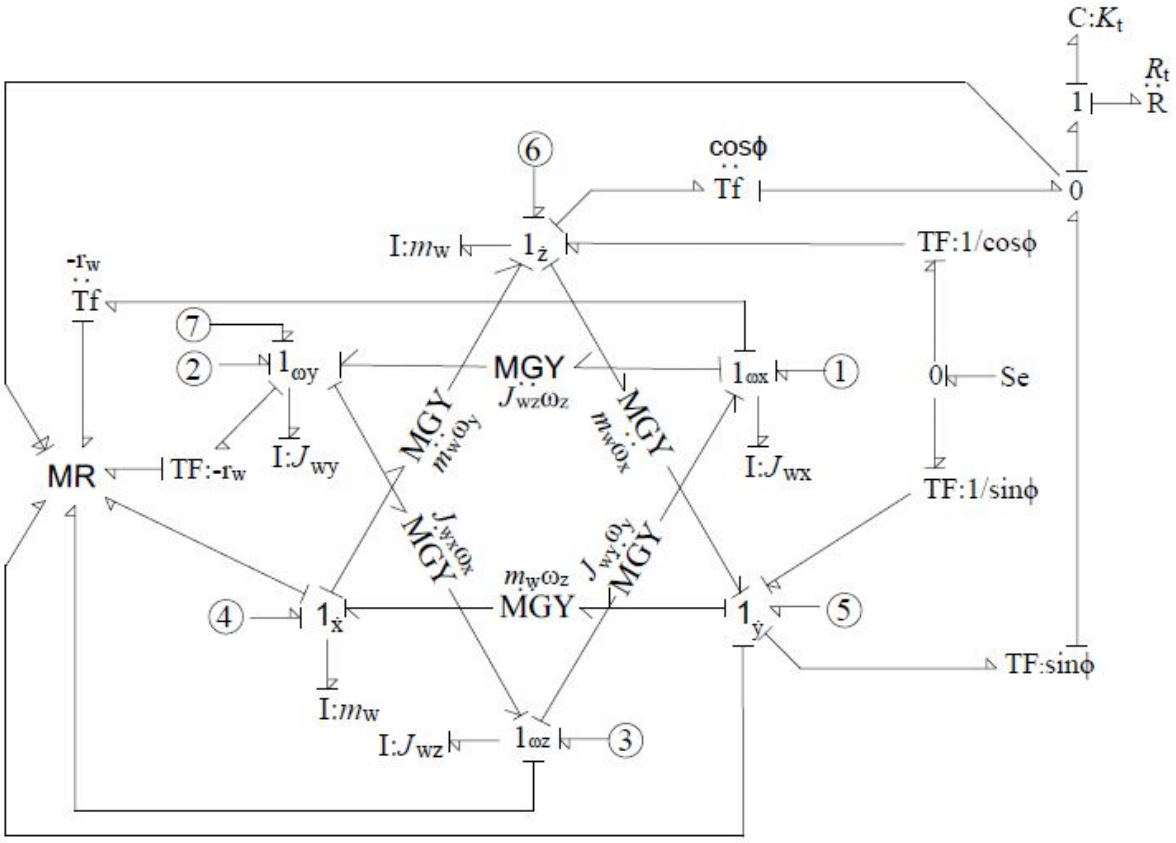

Fig 4.14 Bond graph model of wheel used in reduced four wheel vehicle model.

4.5.4 Parameter values and simulation results

The parameter values used to simulate the full system model and the reduced system model are listed in Table 4.3.

Table 4.3 Parameters used for simulation of four wheel model

Parameter values for four wheel model			
Vehicle Body			
m_v	1600 kg	J_{cx}	260 kg m^2
J_{cy}	1110 kg m^2	J_{cz}	1370 kg m^2
a	0.9 m	*b*	1.5 m
c	0.7 m	*h*	0.1 m
Suspensions			
K_{sx}	10^7 N/m	R_{sx}	2000 N s/m
K_{sy}	10^7 N/m	R_{sz}	2000 N s/m
K_{sz}	80 kN/m	R_{sz}	500 N s/m
K_{stx}	10^7 N m/rad	R_{stx}	2000 N m s/rad
K_{sty}	0 N m/rad	R_{sty}	0 N m s/rad
K_{stz}	10^6 N m/rad	R_{stz}	360 N m s/rad
Wheel			
m_w	15 kg	J_{wx}	0.1 kg m^2
J_{wy}	0.2 kg m^2	J_{wz}	0.1 kg m^2
r_w	0.3 m		
Tyre			
K_t	305 kN/m	R_t	200 N s/m
C_1	1.029	C_2	17.16
C_3	0.523	C_4	0.03
Brake			
σ_{low}	0.2	σ_{high}	0.25
s_g	0.01	k_g	250 N m
r_{bd}	0.15 m	R_{lm}	0.04 N s/m
K_{ca}	10^4N/m	K_{re}	10^6 N/m
l_a	1 m		
Steering Wheel			
J_{stw}	1 kg m^2	δ	0 rad

The full model and reduced model were simulated using the above mentioned parameters. As in our assumption on no steering, the lateral dynamics do not have much of an effect, so the models were compared in terms of their longitudinal dynamics. Initially, the vehicle was at rest and gradually accelerated to a constant velocity. The longitudinal velocity of the vehicle and pitch angle of the vehicle body, were calculated and compared in both the models. Figure 4.15 compares the longitudinal velocities of the models. Figure 4.15(d) shows that high percentage error is present only at the start, when velocity is very low, but absolute error is within limits. A similar error trend is observed in Fig. 4.16, which compares the pitch angle in the vehicle body.

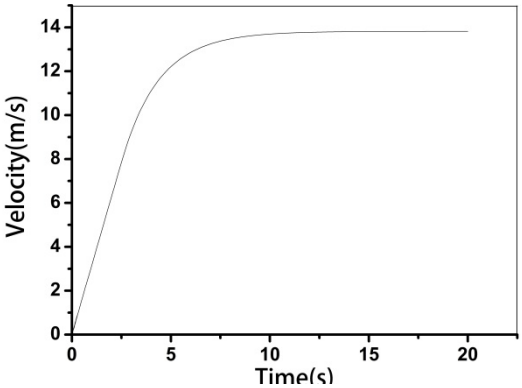

(a) Full model

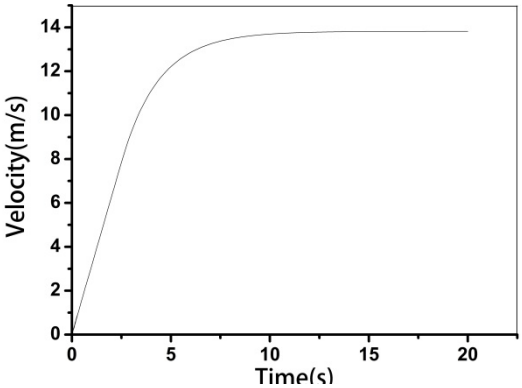

(b) Reduced Model

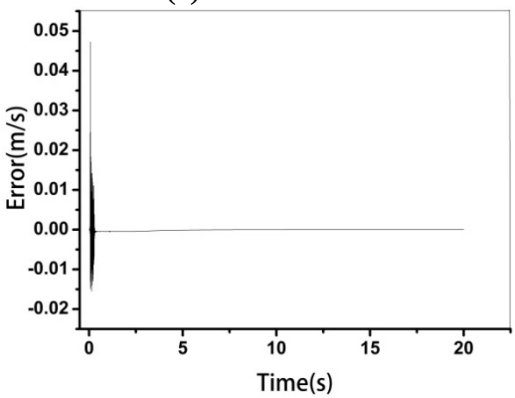

(c) Absolute Error

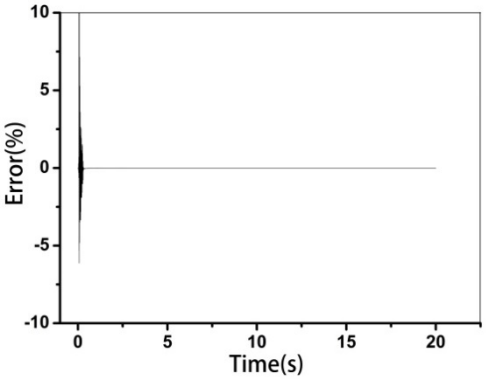

(d) Percentage Error

Fig 4.15 Comparison of longitudinal velocity of full and reduced model

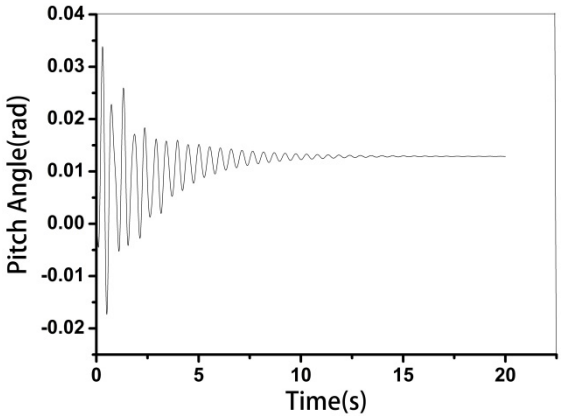

(a) Full model

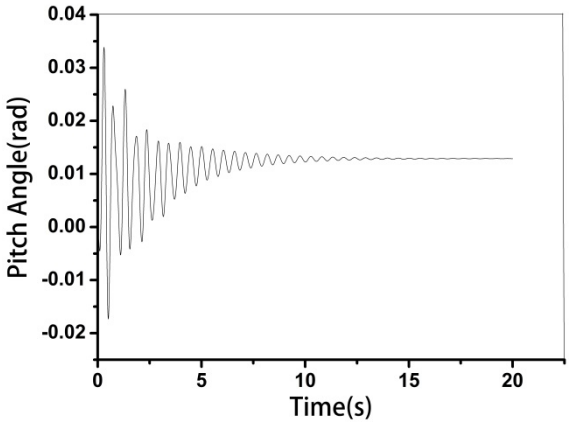

(b) Reduced Model

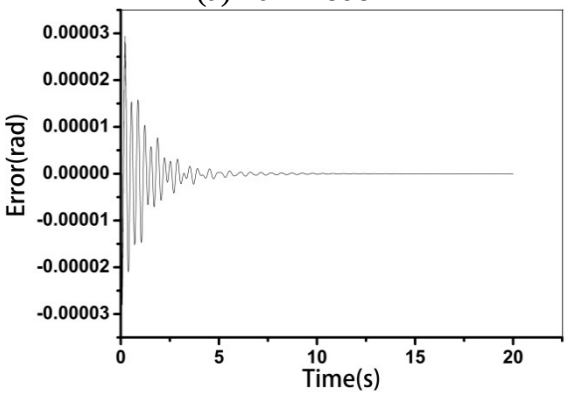

(c) Absolute error

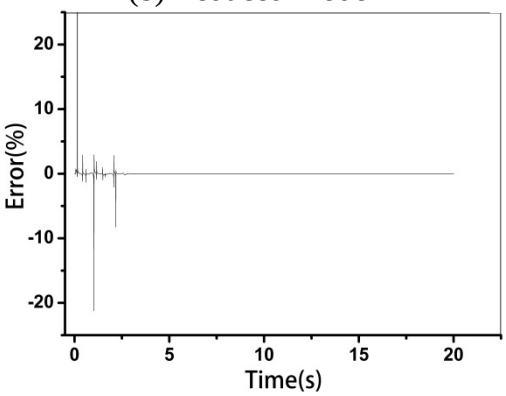

(d) Percentage error

Fig. 4.16 Comparison of pitch angle at vehicle body in full and reduced model

4.6 CASE STUDY III: ABS

4.6.1 Eigenvalue sensitivity technique in ABS

For the purpose of comparison of the Eigenvalue separation and Eigenvalue sensitivity technique, the ABS discussed in Sec. 3.4 was also reduced using the Eigenvalue sensitivity method. Same model and simulation parameters were used to calculate the reduced model as discussed in the previous chapter.

1) The connectivity matrices and characteristic matrices were found for the system. The procedure discussed in section Section 4.2, was applied to find the connectivity.

$$J_{SS} = \begin{bmatrix} 0 & 0 & 0.15 \\ 0 & 0 & -0.15 \\ -0.15 & 0.15 & 0 \end{bmatrix}$$

$$J_{LL} = \emptyset$$

$$J_{LS} = [-1 \quad 0 \quad 0]$$

$$J_{SL} = \begin{bmatrix} 1 \\ 0 \\ 0 \end{bmatrix}$$

2) Then the Eigenvalues of the system were found using Eq.

$$\lambda_1 = -39999.6$$

$$\lambda_{2,3} = -0.0018 \pm 0.0387i$$

3) The effect matrices were found for the system and rounded off to four decimal points. Eq. was used to find the effect matrices. Effect matrix E_{IC} was split into two matrices, Ef_I containing columns corresponding to I-elements in the system and Ef_C containing the columns corresponding to the C-elements in the system.

$$Ef_{\mathrm{I}} = \begin{bmatrix} 0.0006 \\ 0.0006 \\ 0.0006 \end{bmatrix}$$

$$Ef_{\mathrm{C}} = \begin{bmatrix} 0.0103 & 0 \\ 0 & 0 \\ 0 & 0 \end{bmatrix}$$

$$Ef_{\mathrm{R}} = \begin{bmatrix} 257662.4 \\ 0.0024 \\ 0.0024 \end{bmatrix}$$

4.6.2 Reduced model

From the analysis of Eigenvalues, it is observed that second and third Eigenvalue has nearly zero dynamics. Hence, these Eigenvalues are removed. From the analysis of the effect matrices it is observed that, the spring corresponding to the second column of Ef_C can be

removed from the analysis. Hence, the reduced model was obtained, which is shown in Fig. 4.17.

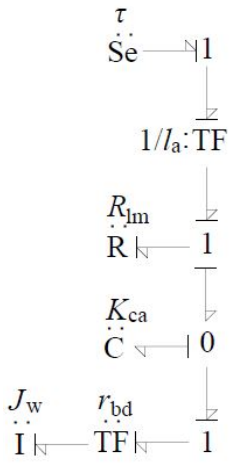

Fig. 4.17 Reduced ABS model from Eigenvalue sensitivity method.

The results from the full model and the reduced model were compared using similar parameter values as in Sec. 3. The comparison is shown in Fig. 4.18.

4.6.3 Simulation Results

From Fig. 4.18, it is observed that the reduced model obtained has high percentage error only when the base value of torque approaches zero. Hence the reduced model is acceptable.

When compared with the results from the reduced model obtained from the Eigenvalue separation method, it is observed that both the models have similar error. But, as the model from Eigenvalue sensitivity matrix is reduced by an order of one, this reduced model is faster to calculate. It is hence concluded that the Eigenvalue sensitivity method is more beneficial and should be preferred over the Eigenvalue separation method.

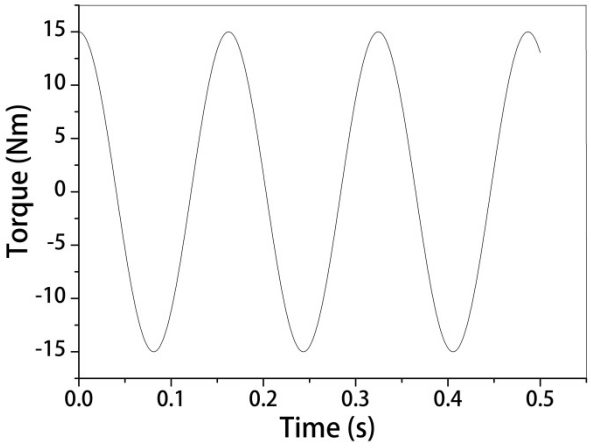

(a) Full model

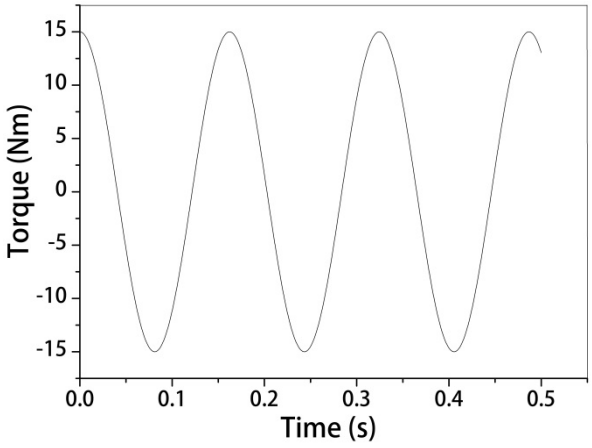

(b) Reduced Model

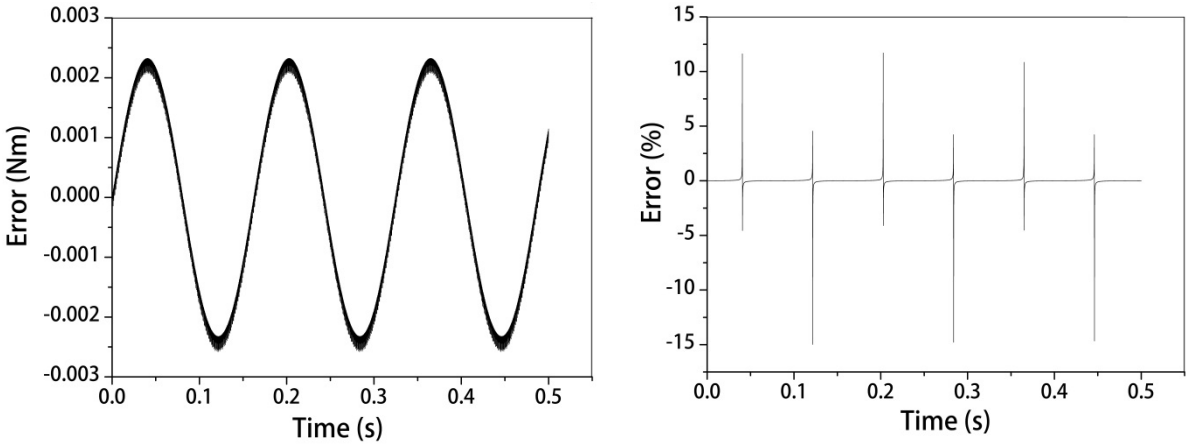

(c) Error (d) Percentage error

Fig. 4.18 Comparison of full model and reduced ABS model from Eigenvalue sensitivity method

CHAPTER 5 CONCLUSIONS

5.1 CONCLUSION

The objective of this thesis was to find out a reduced bond graph models of various vehicle dynamic models by removing some physical components from the analysis to make the calculation easier. The conclusions of the thesis are as follows:

- Both the Eigenvalue separation technique and the Eigenvalue sensitivity techniques are very powerful and are efficient in different situations. The Eigenvalue separation method is very easy to apply and is preferred for small models of if the models has only two of the basic I, C and R elements. But the process becomes difficult to apply for complex models. The Eigenvalue sensitivity method has a major advantage over the previous method that it can be easily automated for major portion. Hence, for complex models, this method is preferred.
- The Eigenvalue separation method gives us a partitioned reduced model which will give correct approximation only during the specified time scale. The Eigenvalue sensitivity matrix on the other hand can provide us with a reduced model for any time scale, the selection of which can be done by selecting the Eigenvalues. In this thesis generalized reduced models were obtained which can be used for all time scales.
- The bond graph model of ABS was reduced using both the Eigenvalue separation method and the Eigenvalue sensitivity method. The reduced models obtained from both methods were accurate but the model obtained from the Eigenvalue sensitivity method had a reduced C-element as compared to reduced R-element from the other process. Hence, Eigenvalue separation method provided us with a better result.
- Bicycle vehicle model in the horizontal plane was reduced was reduced using the Eigenvalue separation method. To linearize the model, the vehicle was simulated on a straight path. The reduction process removed two resistance elements in the reduced model.
- Bicycle model in the vertical plane was reduced with the Eigenvalue sensitivity method. The reduction process led to removal of three I-elements, two C-elements and two R-elements. Hence the order of the model was reduced by five.
- The four wheel vehicle model was reduced using the Eigenvalue sensitivity method. Many non-linear components were linearized by assuming a straight line motion. The

process led to reduction of four I-elements, four C-elements and four R-elements, reducing the model order by eight.

5.2 SCOPE OF FUTURE WORK

Based on the work done in this thesis, the following work is suggested for future:

- The discussed methods are applicable only for LTI systems, so algorithms can be developed to reduce non-linear models using these techniques.
- The Eigenvalue separation method can be modified to handle systems with local damping ratio close to 1.
- As the separation of loop gains depends on the user, a mathematical technique can be developed to find the optimum point of separation for slow and fast sub-systems.

CHAPTER 6 REFERENCES

[1] Davidson AM and Walters IR. Linear system reduction using approximate moment matching. *IEE Proceedings D (Control theory and applications)* 1988; 135: 73–78.

[2] Lalonde RJ, Heartley TT and De Abereu-Garcia JA. Least squares model reduction. *Journal of the Franklin Institute* 1992; 329: 215–240.

[3] Mukherjee A, Karmakar R, and Samantaray AK. *Bond Graph in Modelling, Simulation and fault Identification*. FL: CRC Press, 2006.

[4] Margolis D and Shim T. A bond graph model incorporating sensors, actuators and vehicle dynamics for developing controllers for vehicle safety. *Journal of the Franklin Institute* 2001; 338: 21–34.

[5] Dauphin-Tanguy G, Rahmani A, and Sueur C. Bond graph aided design of controlled systems. *Simulation Practice and Theory* 1999; 7: 493–513.

[6] Gawthrop P. Physical model-based control: A bond graph approach. *Journal of the Franklin Institute* 1995; 332: 285–305.

[7] Bos AM and Tiernego JL. Formula manipulation in bond graph modelling and simulation of large mechatronic systems. *Journal of the Franklin Institute* 1985; 319: 51–65.

[8] Karnopp DC, Margolis DL and Rosenberg RC. *System Dynamics, Modelling and Simulation of Mechatronic System*. New York: John Wiley & Sons, 2000.

[9] Borutzky W. *Bond Graphs-A Methodology for Modelling Multidicsiplinary Dynamic Systems*. San Diego: SCS Publishing House.

[10] Samantaray AK and Ould Bouamama B. *Model based Process Supervision*. London: Springer Verlag, 2008.

[11] Brown FT. Bond graph based simulation of thermodynamic models. *Journal of Dynamic Systems, Measurements and Control* 2010; 132: 064501(1)–064501(3).

[12] Calvo AJ, Caldas CA and Roman JL. Analysis of Dynamic Systems Using Bond Graph Method through Simulink. *Engineering Education and Research using MATLAB.* 2001.

[13] Gillespie TD. *Fundamentals of Vehicle Dynamics*. PA: SAE International, 1992.

[14] Bundell M and Harty D. *The Multibody Systems Approach to Vehicle Dynamics*. London: Elsevier, 2004.

[15] Jazar RN. *Vehicle Dynamics: Theory and Application*. New York: Springer, 2012.

[16] Pacejka HB. *Tyre and Vehicle Dynamics*. Butterworth-Heinemann: Elseveir, 2006.

[17] Singh BR and Singh MK. Dynamic Modelling, Theory and Application using Bond Graph. *SAMRIDDHI- A Journal of Physical Sciences, Engineering and Technology* 2013; 4: 25–36.

[18] Filippini G, Nigro N and Junco S. Vehicle dynamics simulation using bond graph. In: *International Conference on Integrated Modelling and Analysis in Applied Control and Automation*, Buenos Aires, Argentina, 2007.

[19] Deur J, Ivanovic V, Assadin F, et al. Bond Graph Modelling of Automotive Transmissions and Drivelines. In: *7th International Conference on Mathematical Modelling*, Vienna, Austria, 2012.

[20] Burhaumudin MS, Samin PM, Jamaluddin H, et al. Modeling and Validation of Magic Formula Tire Model. In: *International Conference on Automotive, Mechanical and Materials Engineering*, Peneng, Malaysia, 19 May–20 May 2012.

[21] Merzouki R, Ould-Bouamama B, Djeziri MA et al.Modelling and simulation of tire-road longitudinal impact efforts using bond graph approach. *Mechatronics* 2007; 17: 93–108.

[22] You S, Hann J and Lee H. New adaptive approaches to real-time estimation of vehicle sideslip angle. *Control Engineering Practice* 2009; 17: 1367–1379.

[23] Baffet G, Charara A and Lechner D. Estimation of vehicle sideslip, tire forces and wheel cornering stiffness. *Control Engineering Practice* 2009; 17: 1255–1264.

[24] Oniz Y, Kayacan E and Kaynak O. A dynamic method to forecast the wheel slip for antilock braking system and its experimental evaluation. *IEEE Transactions on Systems, Man, and Cybernetics-Part B: Cybernetics* 2009; 39: 551–560.

[25] Silva LI, Magallan GA, De Angelo CH et al. Vehicle dynamics using multi-bond graphs: four wheel electrical vehicle model. In: *34thAnnual Conference of IEEE Industrial Electronics*, Orlando, USA, 10 Nov–13 Nov 2008, papar no. 10415436, pp.2846–2851.

[26] Longoria RG, Al-Sharif A and Patil CB. Scaled vehicle system dynamics and control: a case study in anti-lock braking. *International Journal on Vehicle Autonomous Systems* 2004; 2: 18–39.

[27] Moore B. Principal component analysis in linear systems: Controllability observability and model reduction. *IEEE Transactions on Automatic Control* 1981; 26: 17–32.

[28] Rosenberg RC and Zhou T. Power based model insight. In: *ASME Winter annual meeting on Automated Modeling for Design,* Chicago, USA, 27 Nov–2 Dec 1988, pp. 61–67.

[29] Louca LS, Stein JL, Hulbert GM et al. Proper model generation: an energy-based methodology. In: *3rd International conference on bond graph modeling,* Phoenix, USA, Jan 1997, pp. 44–49.

[30] Louca LS, Stein JL and Rideout DG. Generating proper integrated dynamic model for vehicle mobility using a bond graph formulation. In: *International conference on bond graph modeling,* Phoenix, USA, 2001, pp. 339–345.

[31] Ersal T, Fathy HK and Stein JL. Structural simplification of modular bond-graph models based on junction inactivity. *Simulation Modelling Practice and Theory* 2009; 17: 175–196.

[32] Sueur C and Dauphin-Tanguy G. Bond graph approach to multi-time scale system analysis. *Journal of the Franklin Institute* 1991; 328: 1005–1026.

[33] Orbak AY, Turkay OS, Eskinat E et al. Model Reduction in the physical domain. In: *Institute of Mechanical Engineers. Part I: Journal of Systems and Control Engineering,* 2003, pp. 481–496.

[34] Orbak AY, Eskinat E and Turkay OS. Physical parameter sensitivity of system eigenvalues and physical model reduction. *Journal of the Franklin Institute* 2004; 341: 631–655.

[35] Bera TK, Bhattacharya K, Samantaray AK. Evaluation of antilock braking system with an integrated model of full vehicle system dynamics. *Simulation Modelling Practice and Theory* 2011; 19: 2131–2150.

CURRICULUM VITAE

Manarshhjot Singh did his graduation in Mechanical Engineering from Punjabi University, Patiala in 2012. In the same year he joined SML ISUZU Ltd, Roopnagar, in the Technology Department, where his team was charged with the development of Engine and Transmission assembly line. In 2013, he joined Masters of Engineering Programme Thapar University, Patiala in CAD/CAM Engineering, through GATE 2012. His ME thesis was in the area of physical model reduction for vehicle dynamic models. One paper from his work ‘Physical Model Reduction of Antilock Braking System’ was presented in ‘International Conference on Aeronautical, Robotics and Manufacturing Engineering (ARME'2015)’ at Bangkok, Thailand on June 15-16, 2015. Another journal paper is under prepration.